http://www.icae.jp

Newsletter on Atmospheric Electricity

Vol. 26 • No 1 • May 2015

INTERNATIONAL COMMISSION ON ATMOSPHERIC ELECTRICITY (IAMAS/IUGG)

AMS COMMITTEE ON ATMOSPHERIC ELECTRICITY

AGU COMMITTEE ON ATMOSPHERIC AND SPACE ELECTRICITY

EUROPEAN GEOSCIENCES UNION

SOCIETY OF ATMOSPHERIC ELECTRICITY OF JAPAN

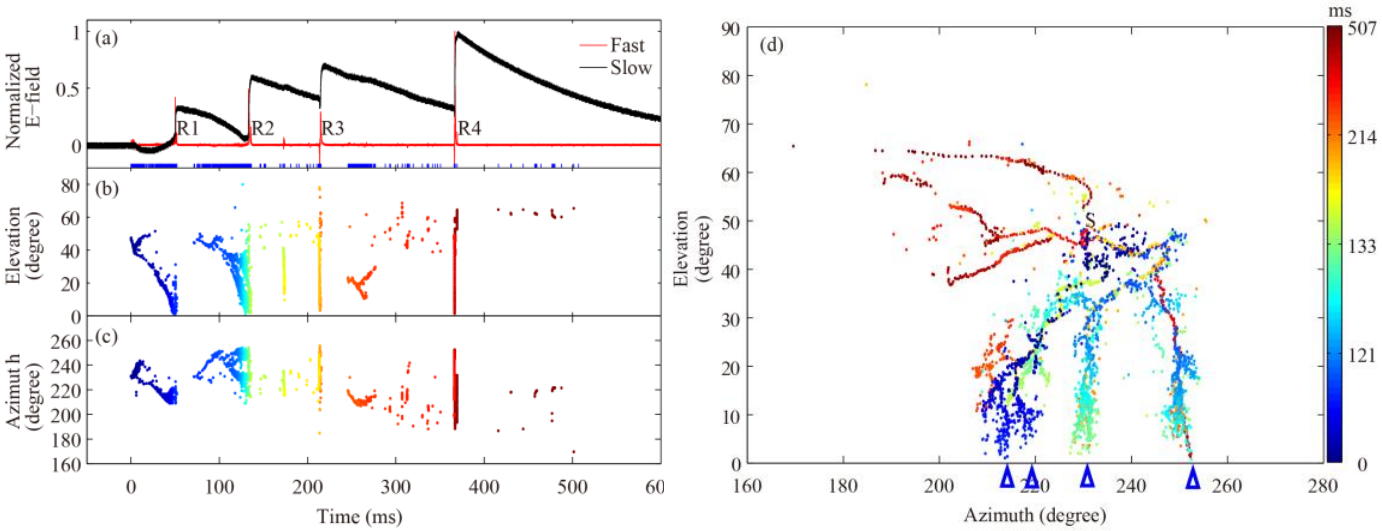

***Comment on the photo above*: A cloud-to-ground lightning discharge with multiple ground terminations viewed by using a VHF radiation location system. During its preliminary breakdown process, two leader channels formed and progressed simultaneously. One of them transformed into a stepped leader which propagated downwards with branches and eventually caused the first return stroke. Interestingly, the second return stroke leader spread along the other channel of the preliminary breakdown, and therefore resulted in a multiple channel flash (MCF). Both of the first and second return strokes themselves are multiple-ground terminations strokes (MGTSs). This figure, including the discharge's animation (an attached file), is provided by Zhuling Sun, Institute of Atmospheric Physics, Chinese Academy of Sciences (CAS), Beijing. Adapted from a paper submitted to JGR by Sun et al., 2015.**

ANNOUNCEMENTS

Datasets on fair weather atmospheric electricity

Hannes Tammet
University of Tartu, Estonia

The DataCite global consortium (https://www.datacite.org) supports archiving of research data and helps to assign to datasets digital object identifiers (DOI). This opportunity is now used uploading four datasets to a safe repository and making the data openly accessible.

Dataset ATMEL2007A
Access http://dx.doi.org/10.15155/repo-1

Annotation:
The dataset of fair weather atmospheric electricity ATMEL2007 (Tammet, 2009) provides scientists and students with a collection of data for exploring the correlations and trends in fair-weather atmospheric electricity, air pollution effects, and trends in global climate. It includes hourly averages of digitally available data from 13 stations including 7 stations of the former World Data Centre network (Dolezalek, 1992). Additional stations are Wank Peak (Germany), Marsta (Sweden), Tahkuse (Estonia), Tartu (Estonia), Hyytiälä (Finland), and Carnegie research ship. The atmospheric electric measurements are accompanied with meteorological and air pollution data. The total amount of included hourly average values is about 12,000,000. New data can easily be imported into the dataset and the excerpts of the data can be exported as traditional tables using the included free software. The web-version of the dataset includes a new tool *ATMEL2007tablemaker* for easy access. Introductory presentation of the dataset is available in the included pdf-documents:

- Introduction to the ATMEL2007A.
- Motivation of the dataset ATMEL2007A.
- Sources of ATMEL2007A data.
- Explanation of data formats in ATMEL2007A.
- Brief overview of the ATMEL2007A data.
- Tools for data management in ATMEL2007A.
- Manual of ATMEL2007tablemaker.

The dataset ATMEL2007A is not designed for direct running via the Internet. Complete package of data, software, explanations, and instructions should be downloaded from the website and operated in the personal computer of the scientist. The working version of the dataset in the user's computer can safely be protected from unauthorized access. This allows expanding the personal version of the dataset with classified private data and the use of the downloaded data as the background in a specific research.

Dataset Nanoion2010_11
Access http://dx.doi.org/10.15155/repo-2

ANNOUNCEMENTS

Annotation:

The positive and negative small and intermediate air ions were routinely measured at Tartu, Estonia (58.373 N, 26.727 E, 70 m a.s.l.) by means of a unique instrument SIGMA (Tammet, 2011). The dataset includes results of a measurement campaign started at 1 April 2010 and finished at 8 November 2011. The dataset presents unique information about nanoparticles up to 7.4 nm in diameter in the atmospheric air (Tammet et al., 2013, 2014). The genesis and subsequent evolution of nanoparticles is a key to understanding the formation of atmospheric aerosols, which is an essential factor of the Earth's climate. The particles are classified according to their size and electric mobility. The full mobility range was logarithmically uniformly divided into 16 fractions. 10 of these fractions include the intermediate ions and 6 include the small ions. Immediately was determined the particle electric mobility while the size was calculated as the mobility equivalent diameter of the particle.

The dataset contains files:

- nanoion2010_11description.pdf – information about the origin of data and structure of the data files,
- nanoion2010_11instrument.pdf – description of the instrument SIGMA used for measuring nanoparticle mobility and size distribution,
- nanoion2010_11hours.xls – hourly averages of nanoparticle distribution according to their mobility and size, complemented with meteorological data,
- nanoion2010_11records.xls – five minute averages of nanoparticle distribution according to mobility and size,
- nanoion2010_11diagrams.ppt – contour plots of nanoparticle size distribution evolution during 147 days,
- nanoion2010_11.zip – compressed package of files for download and offline use on a personal computer.

Dataset Hyytiala08_10aerosol

Access http://dx.doi.org/10.15155/repo-3

Annotation:

The dataset Hyytiala08_10aerosol contains results of routine measurements of atmospheric aerosols carried on in a well equipped boreal research station during 3 years. The particle size range from 3 nm to 15μm is split into 60 fractions and the records of distribution function are presented for 21682 hours of measurements. The dataset provides scientists with a tool for exploring the structure and dynamics of atmospheric aerosol size distribution. Additionally, it can serve as a basis for data analysis exercises for students in field of environmental sciences.

The dataset includes three files:

- Data_Hyytiala08_10aerosol.xls – a spreadsheet, which contains 60 columns of values of the particle size distribution function and 30 columns of complementary variables.

ANNOUNCEMENTS

- Description_Hyytiala08_10aerosol.pdf – detailed description of origin and structure the data. Additionally includes sample diagrams, which illustrate the data and may provoke new ideas for studies on atmospheric aerosol.
- Package_Hyytiala08_10aerosol.zip – a compressed package, which contains both the data file and the description file. The package is to be downloaded to a personal computer, unzipped and used offline.

The dataset was compiled in process of studies on coagulation sink of fine nanoparticles and small ions by Tammet and Kulmala (2014) and can be used for examination of air ion balance in the atmosphere.

Dataset FinEstIon2003_06

Access http://dx.doi.org/10.15155/repo-4

Annotation:

The dataset includes results of simultaneous measurements of positive and negative atmospheric ions in three stations during four years from 2003 until 2006. Atmospheric ions or briefly air ions are charged nanoparticles naturally found in atmospheric air. The genesis and subsequent evolution of particles is a key to understanding the formation of atmospheric aerosols, which is an essential factor of the Earth's climate. The particles are classified according to their size and electric mobility. The particle electric mobility was immediately determined while the size was calculated as the mobility equivalent diameter of the nanoparticle. The small and intermediate air ions were measured at Hyytiälä, Finland (61°51'N, 24°17'E, 180 m a.s.l.), Tartu, Estonia (58.373 N, 26.727 E, 70 m a.s.l.), and Tahkuse, Estonia (58°315'N, 24°555'E, 27 m a.s.l.), while large air ions were measured only at Tahkuse. The air ion measurements are accompanied with basic meteorological data. The dataset is not designed for direct running via the Internet. Complete package of data, software, explanations, and instructions *Finestion2003_06.zip* should be downloaded from the website, unpacked, and operated in the personal computer of the scientist. Full set of measurements is saved as a single table, which can be opened using MS Excel. However, the whole data table is large and analysis of data immediately by means of Excel appears to be inconvenient. Thus the dataset includes a dedicated application, which allows easily extract specific subtables, and presents some extra facilities for manipulation with the time and selecting the variables in modified order. Instructions and descriptions are presented in the document *Finestion_guide.pdf*, which includes references to additional documents and data files.

References

Dolezalek, H. (1992). The World Data Centre on atmospheric electricity and global change monitoring, *Eur. Sci. Notes Inform. Bull*., 92-02, 1–32. http://www.dtic.mil/dtic/tr/fulltext/u2/a249486.pdf.

Tammet, H. (2009). A joint dataset of fair-weather atmospheric electricity. *Atmos. Res*., 91, 194–200. http://dx.doi.org/doi:10.1016/j.atmosres.2008.01.012.

Tammet, H. (2011). Symmetric inclined grid mobility analyzer for the measurement of charged clusters and fine nanoparticles in atmospheric air. *Aerosol Sci. Technol*., 45, 468–479. http://dx.doi.org/10.1080/02786826.2010.546818.

ANNOUNCEMENTS

Tammet, H., Komsaare, K., Hõrrak, U. (2013). Estimating neutral nanoparticle steady-state size distribution and growth according to measurements of intermediate air ions. *Atmos. Chem. Phys.* 13, 9597–9603. http://dx.doi.org/10.5194/acp-13-9597-2013, http://www.atmos-chem-phys.net/13/9597/2013/.

Tammet, H., Komsaare, K., Hõrrak, U. (2014). Intermediate ions in the atmosphere. *Atmos. Res.*, 135–136, 263–273. http://dx.doi.org/10.1016/j.atmosres.2012.09.009.

Tammet, H., Kulmala, M. (2014). Empiric equations of coagulation sink of fine nanoparticles on background aerosol optimized for boreal zone. *Boreal Environ. Res.*, 19, 115–126. http://www.borenv.net/BER/pdfs/ber19/ber19-115.pdf.

CONFERENCES

2015 AGU Fall Meeting

The fall meeting of AGU will be held on 14-18 December 2015, at the San Francisco, California. There will be several sessions associated with atmospheric electricity. For detail, please visit http://fallmeeting.agu.org/2015/.

Announcement of African Centres for Lightning and Electromagnetics Second International Symposium

Lusaka, Zambia - August 11-13, 2015

The Symposium is co-sponsored with the Center for Science and Technology of the Non-Aligned and Other Developing Countries (NAM S&T Centre, www.namstct.org/). This International Symposium will provide a platform for the participants from nations across Africa to learn about lightning hazard related topics, gain insights into strategic interventions and develop appropriate systems / interventions to decrease deaths, injuries and property damage from lightning across Africa.
For more information, please see http://aclenet.org/2nd-symposium.

ANNOUNCEMENTS

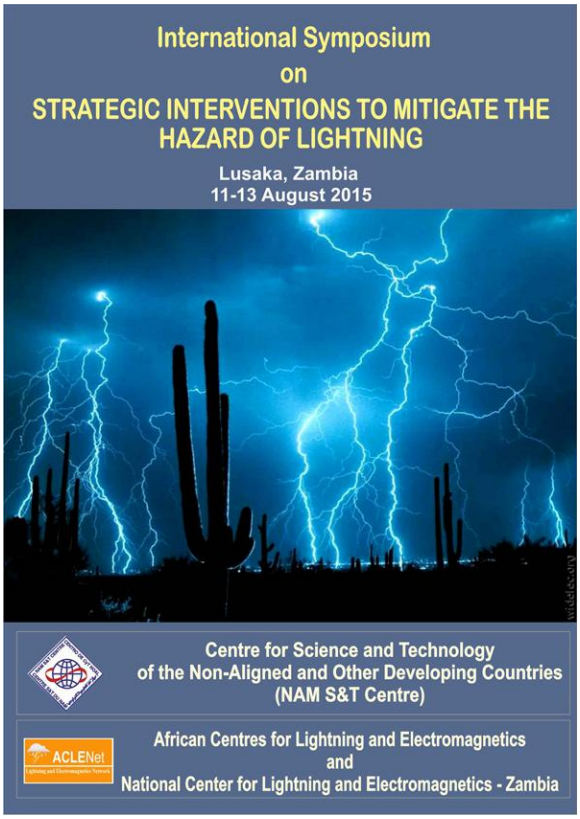

XIII International Symposium on Lightning Protection – SIPDA 2015

Prof. Alexandre Piantini, Chairman of the XIII International Symposium on Lightning Protection (SIPDA 2015), is very pleased to announce the **Call for Papers** of the symposium, which will be held in Balneário Camboriú, Brazil, from 28th September to 2nd October, 2015.

The event is organised by the Institute of Energy and Environment of the University of São Paulo (IEE/USP) with the technical co-sponsorship of the *Institute of Electrical and Electronics Engineers* (IEEE) and support of the National Institute for Space Research (INPE) and the Federal University of Minas Gerais (UFMG).

The aim of the symposium is to present and discuss recent developments concerning lightning modelling and measurement techniques, as well as grounding and lightning protection. The main topics of the symposium are:

1. Lightning Physics, Characteristics and Measurements
2. Lightning Detection and Location Systems
3. Lightning Protection of Substations and Transmission Lines
4. Lightning Protection of Medium and Low Voltage Distribution Lines
5. Lightning Protection of Structures and Installations
6. Lightning Protection of Electronics and Telecommunication Systems

ANNOUNCEMENTS

7. Grounding
8. Lightning Electromagnetic Fields and Electromagnetic Compatibility
9. Testing and Standardisation
10. Lightning-caused Accidents and Injuries

The papers presented at the symposium will be published in the *IEEE Xplore* database. In addition, just like in the previous SIPDA edition, a special issue of the *Electric Power Systems Research* is being planned to publish extended and improved versions of selected papers. The deadline for paper submission (through the symposium website: www.usp.br/sipda) is **June 1st, 2015.**

For further information about the Symposium, please visit the web site at: http://www.usp.br/sipda or contact us through the e-mail sipda@iee.usp.br.

SPECIAL TOPICS

On the electric field sign convention, reversal distance, and the meaning of field components

Vladimir A. Rakov

The purpose of this note is to provide illustrations for the nice article by P. Krehbiel, V. Mazur, and W. Rison concerning a number of topics related to the sign convention for electric field measurements in atmospheric electricity (Newsletter on Atmospheric Electricity, Vol. 25, No. 2, 2014, pp. 5-8). Additionally, the three components, often identified by their $1/R^3$, $1/R^2$, and 1/R distance dependences, of the lightning electric field change are further discussed.

1. Electric field due to cloud charges

Shown in Fig. 1 is the electric field at ground due to an idealized system of three vertically stacked charges (a vertical tripole) in an insulating atmosphere, computed assuming that the middle negative (Q_N) and top positive (Q_P) charges are 7 and 12 km above ground, respectively, each having a magnitude of 40 C, and that the bottom positive charge (Q_{LP}) is at 2 km and has a magnitude of 3 C. An upward-directed electric field is defined as positive (the physics sign convention). As seen in Fig. 1, the total electric field of three vertically-stacked charges in the cloud will have two polarity reversals at the ground, one between 0 and 5 km and the other between 10 and 15 km from the tripole axis. Such field versus distance variation, although model dependent, is qualitatively consistent with the available experimental data. Also shown in Fig. 1 are the contributions to the total electric field from each of the three charges.

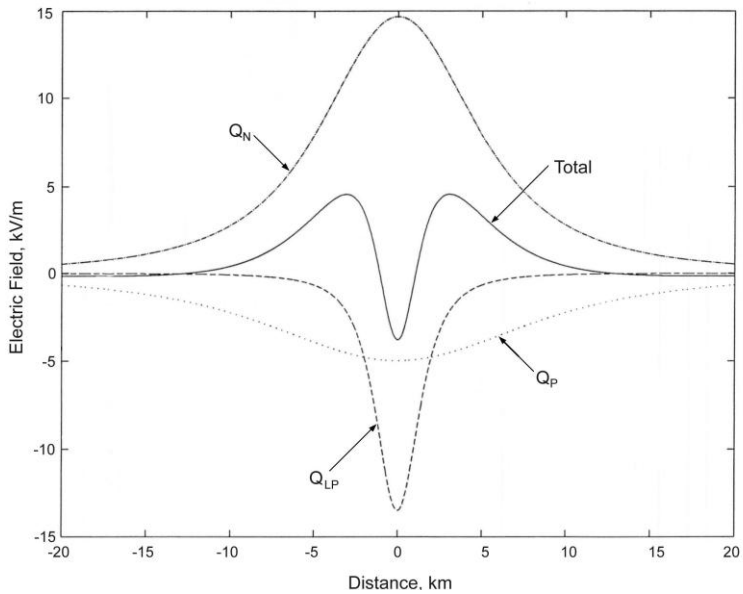

Fig. 1. Electric field at ground due to a vertical tripole, labeled Total, as a function of distance r from the axis (at r = 0) of the tripole. Also shown are the contributions to the total electric field from the three individual charges of the tripole. Electric field changes due to cloud-to-ground and intracloud discharges are shown in Figs. 2 and 3, respectively. An upward directed electric field is defined as positive (physics sign convention). Adapted from Rakov and Uman [2003, Ch. 3].

For the case of two vertically-stacked charges of equal magnitude but opposite polarity there will be only

one reversal distance given by

$$D_0 = \left[\left(H_P H_N \right)^{2/3} \left(H_P^{\ 2/3} + H_N^{\ 2/3} \right) \right]^{1/2} \tag{1}$$

where H_P and H_N are the heights of the positive and negative charges, respectively. Thus, for a positive dipole (positive charge above negative), one might expect the total electric field to be negative at close ranges (because the closer negative charge will dominate the field), while at far ranges it will be positive (because the larger-elevation-angle positive charge will dominate the field). Neither of the reversal distances seen in Fig. 1 is described by Eq. (1), since it has been derived for just two vertically-stacked charges.

2. Net electric field changes due to lightning

In general, an electric field change is the difference between the final electric field (established after an effective charge removal due to lightning) and the initial electric field (produced by the original cloud charge distribution). For any charge that is effectively removed from the cloud, the corresponding change in the electrostatic field is the negative of the contribution of that charge to the initial electric field. If we assume that a negative cloud charge (Q_N) is completely neutralized by a cloud-to-ground discharge, the resultant net electric field change will be negative at all distances, as shown in Fig. 2, because the upward-directed (positive) electric field due to the negative charge (see Fig. 1) disappears; that is, becomes zero. If both the top positive (Q_P) and middle negative (Q_N) charges are neutralized via an intracloud discharge, the resultant net field change as a function of distance will exhibit a polarity reversal, as seen in Fig. 3. Note that the positive field values in Fig. 3 are considerably smaller than negative field values. The polarity reversal occurs because the net field change is the negative of the sum of the contributions to the total electric field, shown in Fig. 1, from these two charges, this sum being positive at close ranges (dominated by the lower negative charge) and negative at far ranges (dominated by the higher positive charge). In other words, for such an intracloud discharge, the electric field change at close ranges is dominated by the reduction of the positive (upward-directed) electric field and at far ranges by the reduction of the negative (downward-directed) electric field.

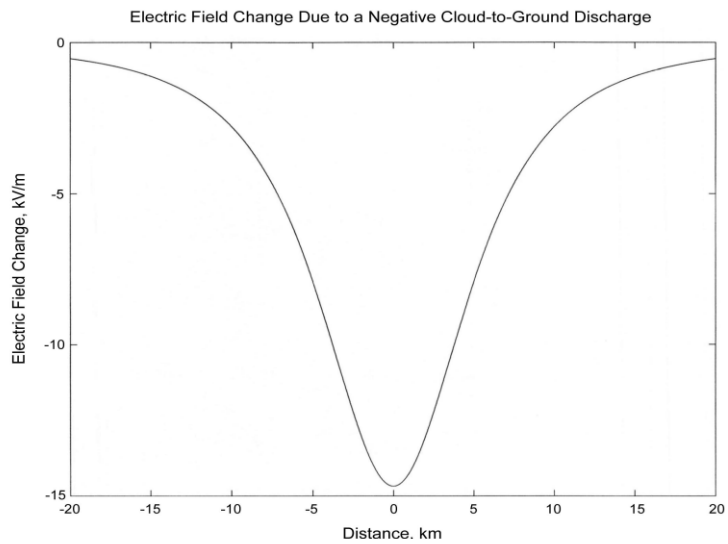

Fig. 2. Electric field change ΔE at ground due to the total removal of the negative charge of the vertical tripole via a cloud-to-ground discharge as a function of distance from the axis of the tripole. Note that

the electric field change at all distances is negative (it is the negative of the curve labeled "Q_N" in Fig. 1). Adapted from Rakov and Uman [2003, Ch. 3].

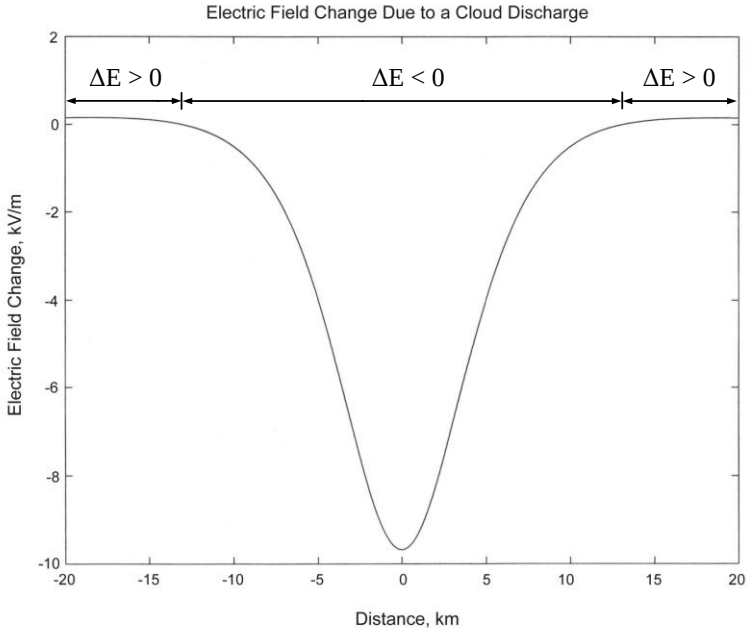

Fig. 3. Same as Fig. 2, but due to the total removal of the negative (Q_N) and upper positive (Q_P) charges via an intracloud discharge. Note that the electric field change at close distances is negative, but at far distances it is positive (it is the negative of the sum of the curves labeled "Q_N" and "Q_P" in Fig. 1). The reversal distance is 13 km. Adapted from Rakov and Uman [2003, Ch. 3].

3. The reversal distance for electrostatic and induction electric field components of a short current element

For an elevated short dipole that is vertical (see Fig. 4), the peak radiation field on the one hand and induction (intermediate) and static field changes on the other hand may have opposite polarities. This follows, for example, from Eq. (A.38) (based on the dipole technique; see Section 4 below) of Uman [1987, p. 329] for the electric field due to a differential vertical current element idz located at height z above perfectly conducting ground. The horizontal distance r at which the static and induction components on the ground reverse their direction is equivalent to the reversal distance of the electrostatic field from an elevated, finite-length vertical dipole (see Eq. (1)).

Motion of positive charge upward (or negative charge downward) produces a radiation electric field change (initial peak) directed downward at all distances, as shown in Fig. 4 (inset). Conversely, for positive charge moving downward (or negative charge upward) the radiation electric field is directed upward. At close distances (i.e., for angle $\alpha > 35.3°$ in Fig. 4), the motion of positive charge upward produces electrostatic and induction field changes directed upward and the radiation electric field change is directed downward, while at far distances (i.e., for $\alpha < 35.3°$), all three electric field components are directed downward.

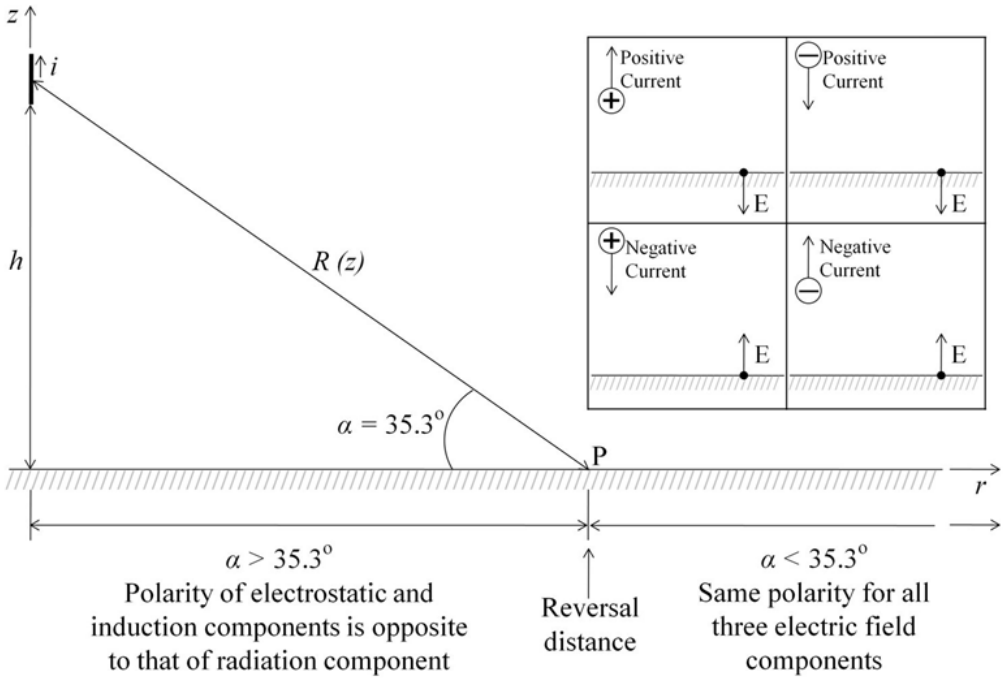

Fig. 4. Illustration of the reversal distance for the electrostatic and the induction field components (dipole technique; see Section 4). Inset shows the direction of the radiation component of electric field vector for different combinations of the charge polarity and the direction of its motion (also the direction for all three components when α < 35.3°). The direction of the electric field vector refers to the initial half cycle of bipolar waveforms. Adapted from Nag and Rakov [2010].

4. Non-uniqueness of electric field components

The three components of an electric field (or the change in that field), referred to as the electrostatic, induction (intermediate), and radiation components, are not unique [e.g., Rubinstein and Uman, 1989]. For example, these components, often identified by their $1/R^3$, $1/R^2$, and 1/R distance dependences, are different for the dipole (Lorentz condition) and monopole (continuity equation) approaches to calculating lightning electric fields. In both approaches, the electric field is found as $\bar{E} = -\text{grad}\varphi - \partial\bar{A}/\partial t$, where φ is the scalar potential and $\bar{A}$ is the vector potential. The expressions for $\bar{A}$ in the two techniques are the same, but those for φ are different: φ is found from $\bar{A}$ using Lorentz condition in the dipole technique, while in the monopole technique it is found from the charge density, which is related to current via the continuity equation.

The two approaches are equivalent; that is, produce identical total fields, although the individual field components may even have different polarities, as seen in Table 1. Note that, in contrast with the more common dipole (Lorentz condition) technique, there is no reversal distance for the $1/R^3$ and $1/R^2$ components in the monopole technique, and that the 1/R component originates only from the time-derivative of magnetic vector potential. (There is another version of the monopole technique [Thottappillil and Rakov, 2001], which yields different $1/R^3$, $1/R^2$, and 1/R components, but identical total fields.) The differences between the field components found using different techniques are considerable at close ranges but become negligible at far ranges.

Table 1. Comparison of E-field components (at ground level) based on dipole (e.g., Uman, 1987) and monopole (Thomson, 1999) techniques for a differential current element idz at height z above ground.

E-field component identified by its distance dependence	Originated from		Polarity	
	Dipole technique	Monopole technique	Dipole technique	Monopole technique
$1/R^3$ (electrostatic)	gradϕ	gradφ	Negative for $\alpha < 35.3°$ Positive for $\alpha > 35.3°$	Negative
$1/R^2$ (induction)	gradφ	gradφ	Negative for $\alpha < 35.3°$ Positive for $\alpha > 35.3°$	Negative
1/R (radiation)	gradφ and $\partial\bar{A}/\partial t$	$\partial\bar{A}/\partial t$	Negative	Negative

φ is the scalar potential (different in the two techniques) and $\bar{A}$ is the vector potential;
$\bar{E} = -\text{grad}\varphi - \partial\bar{A}/\partial t$; $\alpha = \sin^{-1}(z/R(z))$.

For the dipole approach, Thottappillil and Rakov [2001] have noted that the distance dependences are not exactly $1/R^3$, $1/R^2$, and 1/R, because of the additional dependence on $\sin^2\theta$, where $\sin\theta = r/R$, with r and R = f(z) being the horizontal and inclined distances, respectively, between the source and field points. Only when $\sin^2\theta \approx 1$ (at relatively large distances), are the distance dependences exactly $1/R^3$, $1/R^2$, and 1/R.

5. Short channel segment vs. total radiating channel length

The electric field components discussed in Sections 3 and 4 above are defined for a differential current element (an electrically short channel segment), for which the current does not vary along the radiator length. In computing lightning electric fields, the integration over the entire radiating channel (over height z) must be performed at each instant of time, with the inclined distance R being a function of z. As a result, the horizontal distance r = const is often used instead of R = f(z) for evaluating the distance dependence of field components produced by the entire radiating channel.

For the transmission line model [Uman and MacLain, 1969], the sum of electrostatic and induction field components at close ranges and the radiation field component at far ranges each vary approximately as 1/r and each are proportional to the channel-base current [Chen et al., 2015, Table 1]. As the current wave propagation speed v approaches c (speed of light), the approximate close-range equation (derived using only the *electrostatic and induction* field components) and the approximate far-range equation (derived using only the *radiation* field component) converge to the same (exact) equation for the *total* electric field, which is valid for *any distance* from the lightning channel. Thus, for the transmission line model with v = c, the field components lose their significance. Indeed, in this case, the total electric field (and the total magnetic field) at any distance is proportional to the channel-base current and varies as 1/r (even at very

close ranges), as expected for a spherical TEM wave [Thottappillil et al., 2001].

Sometimes (particularly in studying propagation of electromagnetic waves in the Earth-ionosphere waveguide), the entire lightning channel is approximated as an electrically short dipole with i(z,t) = i(0,t). In this case, the radiation field component is proportional to di/dt, while for the more realistic transmission line model, i(z,t) = i(0,t - z/v), where v is the current wave propagation speed, the radiation field component is proportional to the product of i and v. The difference here is similar to the one between a Hertzian (electrically short) dipole and a traveling-wave antenna, and it has important implications for the estimation of peak currents from range-normalized measured peak fields, as done in modern lightning locating systems. Since the field-to-current conversion procedures in those systems are usually developed for return strokes, assuming that the current peak is proportional to the field peak, they may yield incorrect results for short cloud discharges, because (leaving aside other differences between cloud and ground discharges) the field peak for electrically short radiators is proportional to the current derivative peak, not to the current peak [Nag et al., 2011].

References

Chen, Y., Wang, X., and Rakov, V.A. (2015), Approximate expressions for lightning electromagnetic fields at near and far ranges: Influence of return-stroke speed, *J. Geophys. Res. Atmos.*, 120, 2855–2880, doi:10.1002/2014JD022867.

Nag, A. and Rakov, V.A. (2010), Compact intracloud lightning discharges: 1. Mechanism of electromagnetic radiation and modeling, *J. Geophys. Res.*, 115, D20102, doi:10.1029/2010JD014235.

Nag, A., Rakov, V.A., and Cramer, J.A. (2011), Remote Measurements of Currents in Cloud Lightning Discharges, *IEEE Trans. Electromagn. Compat.*, Vol. 53, No. 2, pp. 407-413.

Rakov, V.A. and Uman, M.A. (2003),Lightning: Physics and Effects, Cambridge University Press, 687 p.

Rubinstein, M. and Uman, M.A. (1989), Methods for calculating the electromagnetic fields from a known source distribution: application to lightning, *IEEE Trans. Electromagn. Compat*., 31, 183-189.

Thomson, E.M. (1999), Exact expressions for electric and magnetic fields from a propagating lightning channel with arbitrary orientation. *J. Geophys. Res.*, 104, 22,293-22,300.

Thottappillil, R. and Rakov, V.A. (2001), On different approaches to calculating lightning electric fields, *J. Geophys. Res.*, 106, 14,191–14,205.

Thottappillil, R., Schoene, J., and Uman, M.A. (2001), Return stroke transmission line model for stroke speed near and equal that of light, *Geophys. Res. Lett*., 28, 3593-3596.

Uman, M.A. (1987), The Lightning Discharge, Orlando, Florida: Academic Press, 377 p.

Uman, M.A. and McLain, D.K. (1969), Magnetic field of the lightning return stroke, *J. Geophys. Res*., 74,6899-74,6910.

RESEARCH ACTIVITY BY INSTITUTIONS

Atmospheric Electricity Group (ELAT), Brazil

During the last summer in Brazil, 9 upward lightning flashes have been recorded by high-speed cameras and electric field sensors. Most of these flashes were triggered by nearby +CG flashes. A few were triggered by IC discharges. They initiated from telecommunication towers located in Sao Paulo, Brazil. All processes of the upward flashes were identified using a *Phantom v711* high-speed video camera located at a distance of 5 km from the towers. The frame rate used was 20,000 images per second.

During June and July 2014, 9 upward lightning flashes have been recorded by high-speed cameras, electric field sensors and a lightning mapping array (LMA) in Rapid City, SD.

Saba, Marcelo M. F., Schumann, C.; Warner, T. A.; Helsdon, J. H. and Orville, Richard E. authored a paper titled: "*High-speed video and electric field observation of a negative upward leader connecting a downward positive leader in a positive cloud-to-ground flash*". In this work, published by *Electric Power Systems Research*, we present a well-documented case of a positive cloud-to-ground flash that shows that the pulses observed in the electric field preceding the return stroke are due solely to the upward propagation of a negative connecting leader (see Figure 1 and 2).

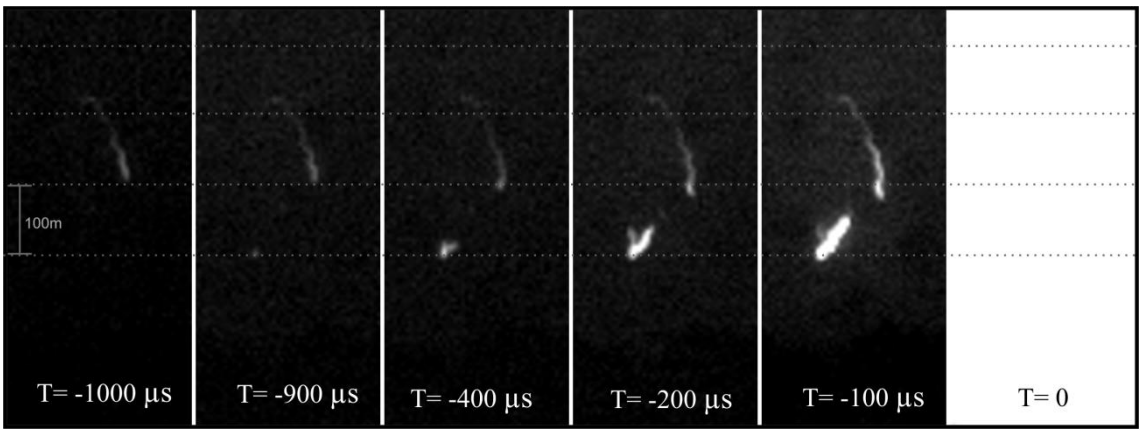

Figure 1 Sequence of video images showing the connection of the negative upward leader (below) with the positive downward leader (above) and the intense luminosity of the return stroke (last image – T=0).

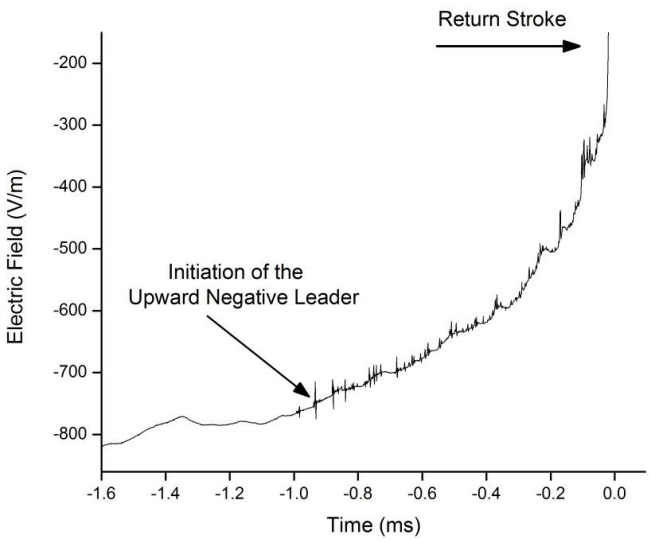

Figure 2 The electric-field plot shows the pulses in the electric field are caused by the upward negative connecting leader.

Colorado State University

Aerosols and the Madden Julian Oscillation

Douglas Stolz, Steven Rutledge, and Jeffrey Pierce Recent research has focused on exploring the regional and temporal variation of the interaction between convective clouds and environmental characteristics. Specifically, our previous research was designed to examine the impact of simultaneous changes in thermodynamics and aerosols on lightning and radar reflectivity throughout the Tropics (e.g., *Stolz et al.*, 2015, in review-JGR). Deep convection (total lightning flash density) was found to be most intense (the greatest) for high CCN concentrations, high normalized CAPE, and shallower warm-cloud depth. One question that arose as a result of that study was whether the aforementioned relationships are robust over all regions or endemic to select regions and seasons.

Our research group participated in the Dynamics of the Madden-Julian Oscillation (DYNAMO) field campaign in the central equatorial Indian Ocean (CIO) during 2011-2012; an objective of this research is to understand changes in behavior of deep convective clouds during different phases of the Madden-Julian Oscillation (MJO, Madden and Julian, 1971, 1972; Wheeler and Hendon, 2004) with respect to changing environmental aerosol concentrations in this region. Our results suggest that horizontal transport of anthropogenic pollutants to the CIO maximizes preferentially during phases 4-6 of the MJO and that convection responds to these periodic infusions of CCN in the boundary layer in later MJO cycles. For example, similar cold cloud feature populations (contiguous areas of cloud-top infrared brightness temperatures < 208 K) are found north and south of the equator in the CIO, yet there is about an order of magnitude more lightning north of the equator on average, where aerosol concentrations are highest (Fig. 1). We hypothesize that different concentrations of CCN in the vicinity of deep convective clouds in the northern and southern portions of the CIO, respectively, contribute to the observed difference in flash rate

and convective vigor as they influence the microphysical evolution of the hydrometeor population. These findings are significant in that the large-scale circulations associated with the MJO may be impacted by asymmetric heating profiles (that are inferred from differences in lightning flash rates and radar characteristics) between the northern and southern regions of the CIO.

On-going research is geared toward extending these results to an eight-year climatology over the CIO. Additionally, a systematic statistical characterization of the cloud-aerosol-thermodynamic interplay over individual regions and seasons is underway. Specifically, we are interested in how lightning responds to aerosols in regions where warm-cloud depth approaches the limit of 0 m, as there were very few samples of these conditions in the TRMM satellite database analyzed by Stolz et al. (2015).

Brett Basarab and Steven Rutledge have continued work on the development of lightning flash rate parameterizations for use in cloud-resolving chemical transport models. Accurate flash rate parameterizations are important to reduce uncertainty in lightning NO_x production in individual thunderstorms, and potentially on the global scale. Typically, lightning parameterizations are based on observed relationships between flash rate and radar-derived storm quantities, such as precipitating ice mass. Since numerous flash rate parameterizations exist in the literature, several existing flash rate parameterizations were tested against a large observational dataset of Colorado thunderstorms from the recent Deep Convective Clouds and Chemistry (DC3) field campaign and from an in-house field project conducted during the summer of 2013. Existing parameterizations were found to inadequately predict flash rate for the sampled storms, with mean error in excess of 20%. Differences from observed flash rates for some individual storms were even higher, suggesting that existing schemes could be introducing significant error in predicted flash rates when applied in cloud-resolving models.

The group has therefore focused recently on improving flash rate parameterization schemes using this Colorado thunderstorm dataset. Robust quantitative relationships ($R^2 \sim 0.85$) were found between lightning flash rate and bulk storm parameters including the graupel echo volume, 35-dBZ volume, and precipitating ice mass within the mixed-phased region of storms (-5 ℃ to -40 ℃). When these relationships were tested against the same storms, observed flash rate trends were predicted well. The mean error over all sampled Colorado storm volumes was 12.7% for the 35-dBZ volume scheme, representing significant improvement over existing schemes. Parameterizations based on updraft intensity such as updraft volume were also modified, but updraft intensity metrics were found to correlate significantly less well to flash rate for this sample. The 35-dBZ volume scheme was tested on a much larger dataset containing reflectivity volumes and LMA-derived flash rates for over 4000 individual storm cells in four different regions: northeast Colorado, central Oklahoma, northern Alabama, and in the vicinity of Washington, D.C. The VOL35 scheme was found to perform very well when applied to this large dataset, with a mean difference between observed and predicted flash rates of 9.1%. This result is encouraging for the potential implementation of this scheme into cloud-resolving models, and it is recommended that this scheme be further tested on large radar datasets.

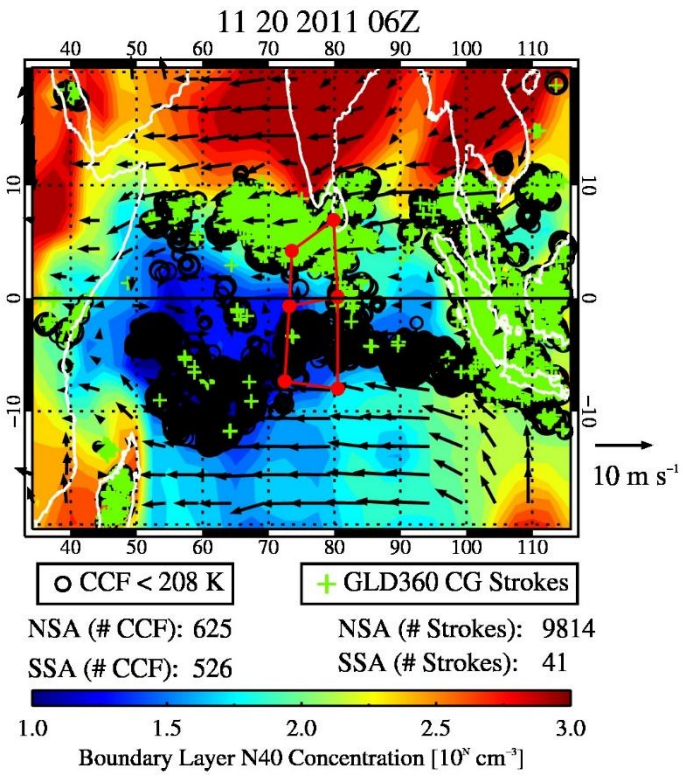

Fig. 1. Boundary layer N40 (CCN) concentrations from the GEOS-Chem transport model (shaded, logarithmic scale), cold cloud features (CCF; IR T_b < 208 K) observed by METEOSAT-7, 925 hPa winds from MERRA reanalysis, and cloud-to-ground (CG) lightning from GLD360 (green plus; Vaisala) at 6:00Z on 20 November 2011. The number of CCFs and CG flashes have been summed over a six-hour period for the northern sounding array (NSA; 0-6^{0}N, 65-85^{0}E) and southern sounding array (SSA; 0-6^{0}S, 65-85^{0}E), respectively.

Indian Institute of Tropical Meteorology

A new tool for predicting drought: An application over India.

Atmospheric electrical columnar resistance (R_c) has been calculated using the aerosol optical depths derived from the satellite aerosol measurements and the model (MERRA) derived planetary boundary layer heights. The R_c varies with the number concentration of aerosols and their vertical distribution on account of vertical convection. The Bay of Bengal (BB) is a region of intense convection. Further, atmospheric events such as ENSO (El Niño Southern Oscillations), IOD (Indian Ocean Dipole) change the global circulations by changing centers of convection and the source regions of aerosols. These changes affect the Indian rainfall as well as the R_c over the BB.

Two new methods for the drought prediction have been developed and applied over India using the calculated R_c over the region (14.5 °N – 19.5 °N; 85.5 °E - 90.5 °E) of the BB. The lead time for the drought prediction is 6-8 months. As the required satellite data for the period January 1993 to July 1996 are not available, both of these methods have been applied for the periods 1981-1990 and 2001-2013 separately (total 23 years) and have

been found to work successfully. The association between the All India Rainfall (*AIRF*) and this new predictor *i.e.*, the atmospheric electrical columnar resistance R_c has also been found on the sub-regional scale. From the analysis, generally, a long period rising trend in the aerosol concentration over the BB causes weak monsoon over India but that for a short time *i.e.*, in pre-monsoon period strengthens it. Thus, the results show that the atmospheric conditions over the BB alone are sufficient to predict the drought over India as a whole. (the paper is open access and the necessary figures depicting more details are accessible online).

The above paper is also available at the following link:

http://www.nature.com/srep/2015/150108/srep07680/full/srep07680.html

Neutral Cluster Air Ion Spectrometer Laboratory, Devendraa Siingh

Continuous measurement of atmospheric ions from Neutral Cluster and Air Ion Spectrometer (NAIS) is going in the premises of Indian Institute of Tropical Meteorology, Pune from 2010 along with SMPS. The example of the new particle events are shown in Figure 1. The main objective of this measurement is to study the generation mechanism of new particle formation. Data of ion concentrations and aerosol size distributions have been analyzed and published in International Journal. We have been also participating in different field experiment for the measurements of ion and aerosol from time to time. Our group's working on the problem of solar activity, lightning and climate issues, Global electric circuit, Thunderstorm and lightning, sprites etc.

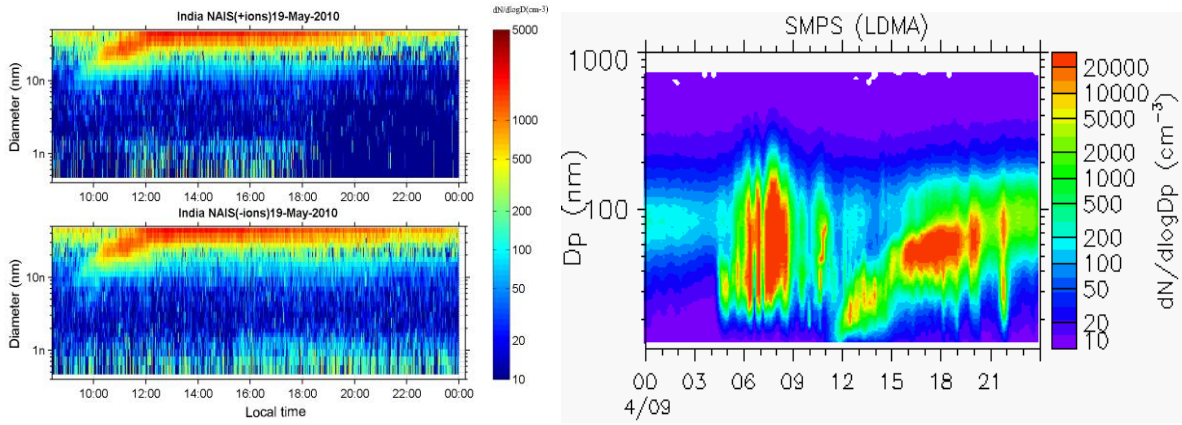

Figure: 1. Neucleation events observed from NAIS and SMPS at Tropical station Pune.

Israel Atmospheric Electricity Group (Tel Aviv University and Interdisciplinary Center)

Yoav Yair and Colin Price continue their studies on fair weather electricity in Israel. With graduate student Roy Yaniv, and new fair weather E-field sensor and Jz current sensor were placed at the Mt. Hermon Cosmic Ray Observatory. our measurements of the diurnal potential gradient show a reasonable agreement with the Carnegie Curve, although we often also see a local midday

peak in Ez, similar to what has been observed in other continental sites. The Ez curves have been compared with global thunderstorm clusters (Mezuman et al., 2014) to determine the contribution of global thunderstorm cells to the fair weather Ez profile.

Graduate student Israel Silber has found that often the vertical magnetic field from distant lightning (in the ELF and VLF ranges) is very large, unlike the theoretical predictions that the vertical magnetic field should be negligible compared with the horizontal fields. The existence of significant vertical magnetic fields has importance in magnetic direction finding for lightning networks, where the vertical magnetic field is often ignored. Another study by Israel Silber shows a clear semi-annual oscillation (SAO) in the narrow band VLF amplitudes detected from VLF transmitters. These signals reflect oscillations in the lower D-region on the SAO primarily at night. Whether the source of this SAO at night is a top-down or bottom-up phenomenon is still unclear. But the SAO is also seen clearly in the airglow layer in OH emissions.

Graduate students David Applbaum and Gil Averbuch are using infrasound to study thunderstorms and sprites in the eastern Mediterranean. We have managed to detect the infrasound signatures of sprites that were detected by the ILAN project optical observations of sprites. In addition to the experimental detection of infrasound, Gil has developed a ray-tracing model of infrasound in the atmosphere to simulate the propagate of the infrasound from the sprites to our observation station in northern Israel.

Graduate student Gal Elhalel continues to work on the link between the Schumann resonances and biological systems. We are performing experiments in a microbiology lab with heart cells from rates (cardiac myocytes). We have found some very interesting results related the the influence of weak SR fields (7.8 Hz) on the cells. Results are being prepared for publication. Masters students Shay Frenkel and Maayan Harel are using the WWLLN data to investigate thunderstorm links to hurricane development (Shay) and climate change (Maayan). The studies are based on the recent paper published by former student Keren Mezuman (Mezuman et al., 2014 in Environmental Research Letters).

Daria Dubrovin has completed her PhD thesis on planetary sprites under the guidance of Yoav Yair and Colin Price, and the help of Ute Ebert from the Netherlands. The thesis and PhD have been approved by Tel Aviv University. Congratulations Daria. Hofit Shahaf has just completed her MSc on magnetic precursors to earthquakes. While we have not detected any significant precursors (maybe because there were no significant earthquakes) we did find some interesting hints of links between magnetic fields and seismic activity.

Finally, a recent publication on hurricane genesis, and the link with African thunderstorms was published last month: Price et al., 2015 in GRL.

Laboratory of Lightning Physics and Protection Engineering (LiP&P), Chinese Academy of Meteorological Sciences (CAMS), Beijing, China

Progress of 2014 Guangdong Comprehensive Observation Experiment on Lightning Discharge (GCOELD)

The 9th GCOELD, carried out in Guangzhou from

May 6 to Aug 28, 2014, has got lots of achievements. The experiments in 2014 focused on the observation of triggered lightning and natural lightning (including tall-object lightning). 15 lightning flashes, including 45 return strokes, have been triggered successfully. The synchronous observation data, including current, electromagnetic signal, optical radiation and high speed video, were acquired. Beside the basic measurement data, the precursor signal data based on large buffer capacity were also obtained. As for the observation of natural lightning, the synchronous observation platform of multiband lightning signal has been further improved based on the fast recording technology and high-accuracy timing technology. The LF and HF electromagnetic signal, VHF radiation signal, optical radiation and high speed video have been detected, triggered and digitized automatically. At the same time, the observation system of electric field change with high-sensitivity has been built and operated continuously. By the end of 2014, we had recorded a lot of multiband and continuous data with lightning discharge. As for the observation of tall-object lightning, we set up some new observation systems, including slow/fast antennas with large detection range and total-sky lighting channel imager. More than 50 tall-object lightning flashes were captured in 2014.

Fig.1 The field experiment site for triggered lightning in Guangdong（left）and a successful triggered lightning(right)

Occurrence regularity of CPT discharge event in negative cloud-to-ground lightning

Chaotic pulse trains (CPT) as electric field pulses in microsecond and sub-microsecond scale have been observed during discharge process of lightning in recent years. Due to the erratic nature in initial polarity, pulse width, pulse separation and pulse amplitude for CPT event, it has been paid more attention. The research about CPT has mainly focused on that prior to subsequent strokes which often is called ‘chaotic leader’. However, we have found that CPT can also appear at other locations in a discharge process of lightning, such as before the first return stroke and after the last return stroke. Up to now, the research on occurrence regularity of CPT is still not adequately detailed.

The occurrence regularity of CPT during negative cloud-to-ground (CG) flashes has been analyzed in detail by the data of electric field change in six thunderstorms observed during the comprehensive observation experiment on lightning discharge in

Guangdong in 2012. The results show that CPT event is a prevalent phenomenon throughout negative CG lightning discharge process. As a statistical result, 243 times of CPT appear out of 323 negative CG flashes. It may occur after the last return stroke (defined as CPT-a), before the first return stroke of a negative CG (defined as CPT-b), as well as between the return strokes (including CPT-c and CPT-i). Thereinto, CPT-c connects with subsequent strokes, and CPT-i occurs between return strokes in a certain interval. 66.7% of the total subsequent strokes are accompanied by CPT-i and CPT-c. CPT-a is more inclined to occur during the lightning with 1-3 return strokes and the probability of total occurrence is 11.5% of the total last return strokes. CPT-b events are extremely rare in the whole discharge process of negative CG flash, and only 2 cases are found. In addition, it can be found that the majority of CPT-i and CPT-a superimpose on the K change. The percentage is 69.7%. Further, based on the electrical field waveforms and the location results of the radiation sources, case study of CPT-i and CPT-c shows that the propagation speeds of CPT-c and CPT-i are similar to those of the speed of dart leaders. The occurrence of the CPT-c and CPT-i in the two cases is associated with the development of dart phase leaders.

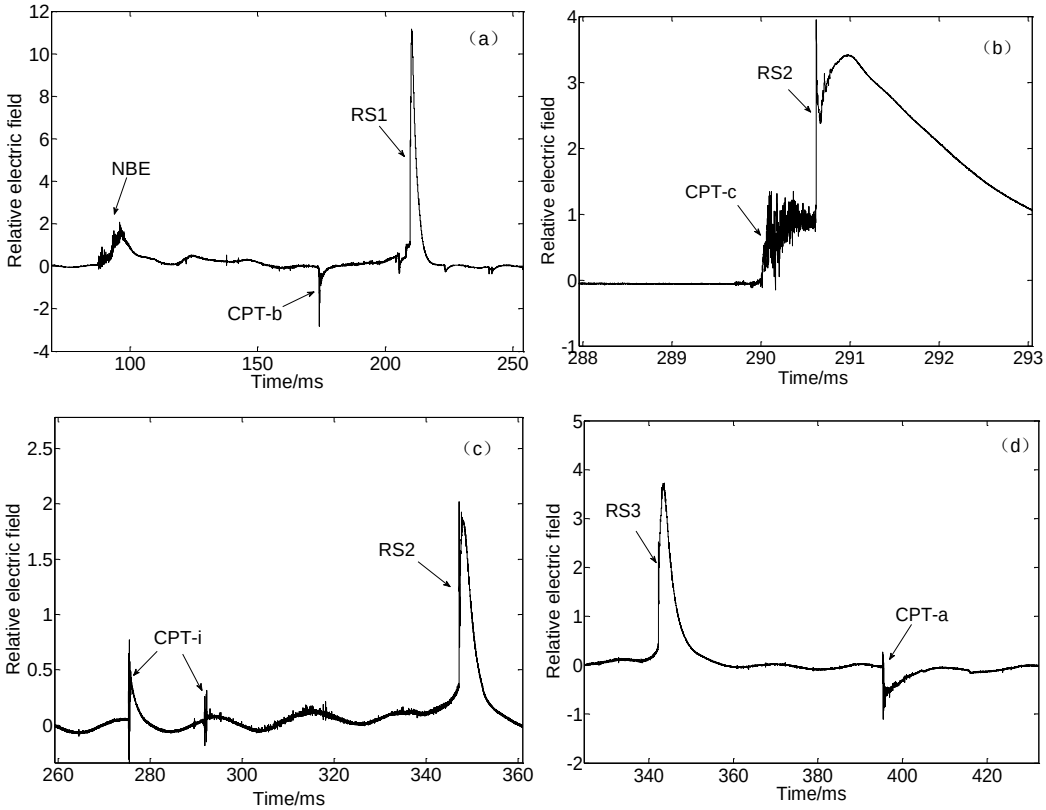

Fig.2 Four types of CPTs in negative CG lightning (a) CPT-b, (b) CPT-c, (c) CPT-i, (d) CPT-a

Optical progression characteristics of an interesting natural downward bipolar lightning flash

Bipolar lightning, in which both positive and negative charges are transferred to the ground in a single lightning flash, have been reported by many authors. However, downward bipolar lightning flashes were rarely observed. Using high-speed cameras, Lightning Attachment Process Observation Systems, and fast and slow electrical antennas, we documented a downward bipolar lightning flash that contained one first positive

stroke with a peak current of 142 kA and five subsequent negative strokes hitting on a 90 m tall structure on 29 July 2010 in Guangzhou City, China. All the six strokes propagated along the same viewed channel established by the first positive return stroke. The leader which preceded the positive return stroke propagated downward at a two-dimensional (2-D) speed of 2.5×10^6 m/s without any branches and exhibited stepped luminosity pulses. An upward connecting leader with a length of about 80m was observed in response to the downward positive leader. The 10–90% rise times of the return strokes' optical pulses ranged from 2.2 μs to 3.2 μs, while the widths from the 10% wave front to the 50% wave tail ranged from 56.5 μs to 83.1 μs, and the half peak widths ranged from 53.4 μs to 81.6 μs. All the return strokes exhibited similar speeds, ranging from 1.0×10^8 m/s to 1.3×10^8 m/s. Each of the return strokes was followed by a continuing current stage (CC). The first positive stroke CC lasted more than 150 ms, much larger than all the subsequent negative stroke CC, ranging from 13 ms to 70 ms.

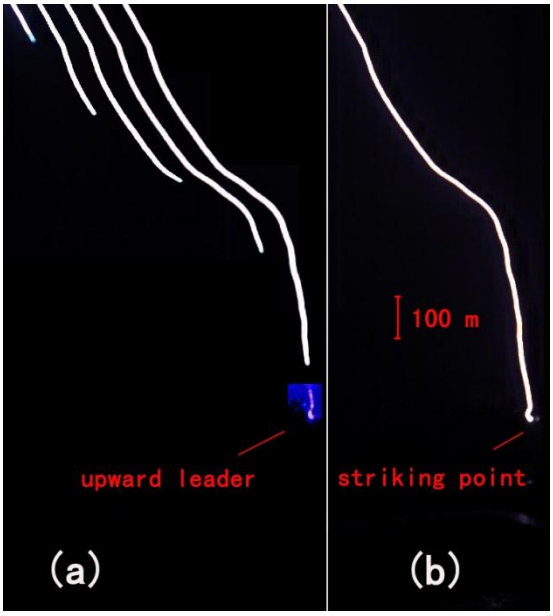

Fig. 3. Images of downward positive leader and upward negative leader captured by a high-speed camera at sampling rate of 10000 fps. (a) for the five images before the R1. (b) for one image of the lightning channel after the R1. The brightness and contrast of the upward negative leader are enhanced for a better view.

Simulation of the electrification of a tropical cyclone using the WRF-ARW model: An idealized case

As a devastating weather system, the tropical cyclone (TC) and its dynamical and microphysical characteristics have long been of interest. It is also found that lightning activity is associated with the formation and development of TCs. The charge structure is the bridge between lightning activity and the dynamical and microphysical characteristics of TCs. This study makes an attempt to illustrate the evolution of the charge structure of TCs.

Evolution of the electrification of an idealized TC is simulated by using the Advanced Weather Research and Forecasting (WRF-ARW) model. The model was modified by addition of explicit electrification and a new bulk discharge scheme (WRF-Electric). The characteristics of TC lightning is further examined by analyses of the

electrification and the charge structure of the TC. Results indicate that the TC eyewall generally exhibits a negative dipole charge structure with negative charge above the positive. In the intensification stage, however, the extremely tall towers of the eyewall may exhibit a normal tripole structure with a main negative region between two regions of positive charge. The outer spiral rainband cells display a simple positive dipole structure during all the stages. It is further found that the differences in the charge structure are associated with different updrafts and particle distributions. Weak updrafts, together with a coexistence region of different particles at lower levels in the eyewall, result in charging processes that occur mainly in the positive graupel charging zone (PGCZ). In the intensification stage, the occurrence of charging processes in both positive and negative graupel charging zones is associated with strong updraft in the extremely tall towers. In addition, the coexistence region of graupel and ice crystals is mainly situated at upper levels in the outer rainband, so the charging processes mainly occur in the negative graupel charging zone (NGCZ).

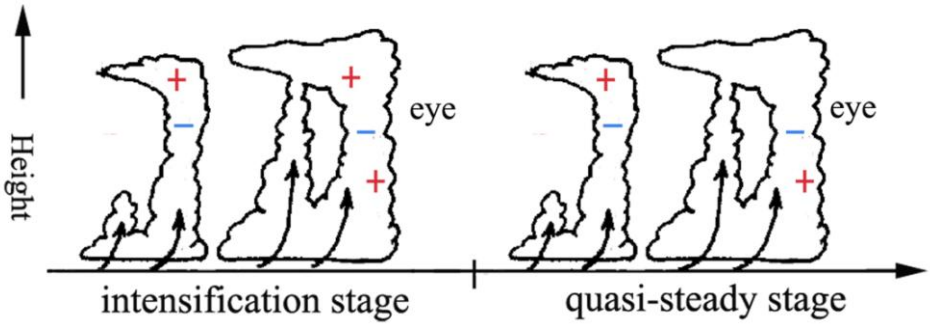

Fig.4. Evolution of the charge structure of a TC during different stages of the TC development.

Relationship between lightning activity and tropical cyclone intensity over the northwest Pacific

Lightning data from the World Wide Lightning Location Network along with tropical cyclone (TC) track and intensity data from the China Meteorological Administration are used to study lightning activity in TCs over the Northwest Pacific from 2005 to 2009, and to investigate the relationship between inner core lightning and TC intensity changes. Lightning in TCs over the Northwest Pacific is more likely to occur in weak storms at tropical depression (10.8–17.1 m s^{-1}) and tropical storm (17.2–24.4 m s^{-1}) intensity levels, in agreement with past studies of Atlantic hurricanes. The greatest lightning density (LD) in the inner core appears in storms undergoing an intensity change of 15–25 m s^{-1} during the next 24 h. Lightning is observed in all storm intensity change categories: rapid intensification (RI), average intensity change (AIC), and rapid weakening (RW). The differences in LD between RI and RW are largest in the inner core, and the LD for RI cases is larger than for RW cases in the inner core (0–100 km) (Fig. 5). Lightning activity there, rather than in the outer rainbands, may be a better indicator for RI prediction in Northwest Pacific storms. There was a marked increase in the lightning density of inner core during the RI stage for Super Typhoon Rammasun (2008). Satellite data for this storm show that the RI stage had the highest cloud-top height and coldest cloud-top temperatures, with all the minimum black body temperature values being below 200 K in the inner core.

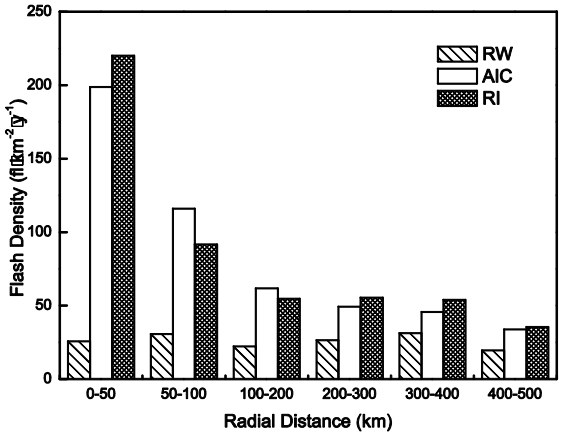

Fig. 5. LD for RW, AIC and RI cases as a function of radial distance from the TC center.

Lightning research group of Gifu University (Gifu, Japan)

A dozen of self-initiated and other-triggered upward lightning discharges from a windmill and its lightning protection tower have been successfully mapped by using a 9 station LMA from New Mexico tech in the coastal area of the Sea of Japan during the last winter. Wang at al. is going to report 7 of the upward lightning occurred during a period of about 3 hours at the coming APL at Nagoya (APL 2015). At least 3 of the 7 upward lightning were triggered by the following discharge processes of nearby positive return strokes. One of the upward lightning is a bipolar discharge which clearly transferred lower negative charge at the height of about 2 km and upper positive charge at about 4 km to the ground. All the remaining 6 upward lightning transferred only lower negative charge at about 1-2 km to the ground. One of the parent storm cells exhibited a typical positive dipole charge structure with its lower negative charge at about 1 or 2 km and its upper positive charge at about 3 or 4 km, while the remaining two parent storm cells exhibited complicated charge structures.

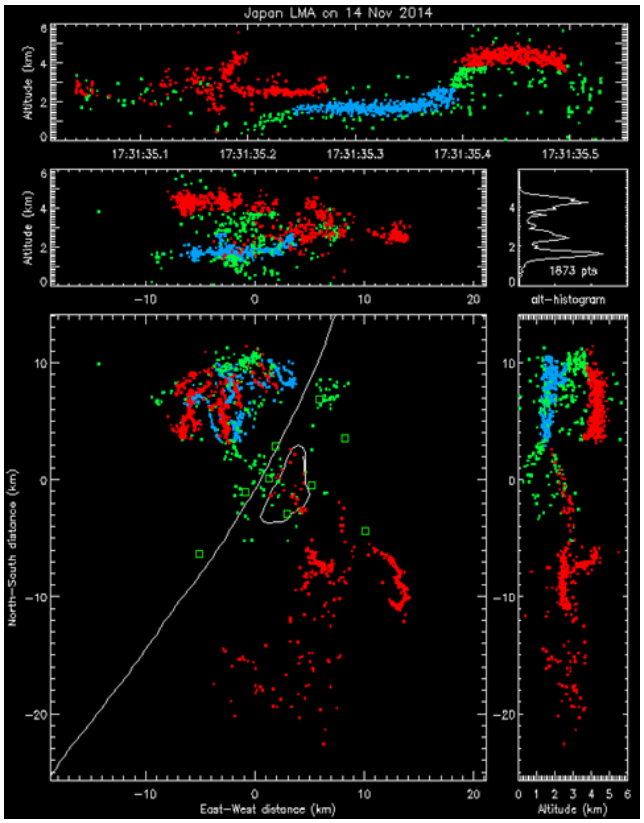

Figure 1 Bi-level structure of charge neutralized by a bipolar other-triggered upward lightning discharge. Red is positive charge region and blue is negative charge region.

RESEARCH ACTIVITY BY INSTITUTIONS

Research Centre for Astronomy and Earth Sciences Geodetic and Geophysical Institute (GGI), Hungarian Academy of Sciences

Earle Williams has visited GGI, Sopron from MIT for a three-month period in the scope of Distinguished Guest Scientist Fellowship Program of the Hungarian Academy of Sciences and participating in several projects involved with atmospheric electricity.

The northeastern coastline of South America is the occasional initiator of long squall lines that propagate to the southwest across the full extent of the Amazon basin to the Andes. The fortuitous circumstance that this coastline orientation is also perpendicular to the great circle path linking the Nagycenk ELF observatory with the South American lightning 'chimney' provides for the possibility of distance-confined lightning activity in this continental source region when such squall lines occur. Confined lightning in the vicinity of the nodal crossing distance (10 Mm) for the fundamental Schumann resonance mode can lead to large variations in modal frequency on the diurnal time scale. Gabriella Sátori and Earle Williams have obtained a comprehensive list of squall lines in South America from Julia Cohen that will be used to identify singular behaviors in the diurnal frequency records at Nagycenk on this basis.

As a follow on to the study of the effects of solar X-radiation on the Schumann cavity on the 11-year solar cycle (Sátori et al., 2005), a study has now been undertaken to understand similar effects on the much shorter time scale of days, during the Halloween Day event of October-November 2003 in which a similar change in X-radiation occurred and for which multiple SR station data are available (Nagycenk, Hungary; Parkfield, CA; Mitzpe Ramon, Israel and West Greenwich, Rhode Island).

Another TLE observation season has been conducted successfully by researchers of the Research Group of Atmospheric Electrodynamics and Chemistry in the Geodetic and Geophysical Institute, Research Centre of Astronomical and Earth Sciences, Hungarian Academy of Sciences. TLE observational facilities in Hungary have been extended by a new station in Baja, south Hungary. The new station allows observations over the Adriatic Sea and over a greater part of Italy, as well as above Macedonia, Albania, and possibly even northern Greece. Members of the research group utilized optical observations of TLEs from previous years in studying meteorological characteristics of sprite producing thunderstorm systems in Central Europe (Odzimek et al., 2014), and above Hungary in particular (Brockhauser et al., 2014, Bór et al., 2014). A peculiar case of sprite sequence including a secondary 'troll' jet event was analyzed in detail together with Polish colleagues (Mlynarczyk et al., 2014). Results demonstrate how effectively current moment variations deduced from ELF electromagnetic measurement can be used in finding out more about the electric environment of these high altitude electrical discharges. Among various effects of lightning strokes, the signature left in seismic records was studied too (Kiszely et al., 2014). Such signatures may be used as a novel tool to study the properties of lightning strokes.

Coupling mechanisms have been studied between the thunderstorms and ionospheric sporadic E-layer based on ionosonde measurements at Pruhonice near Prague and in the Szécshenyi István Geophysical Observatory, Hungary. Both the superposed epoch method and individual case studies were applied. A decrease of the critical

frequency of the sporadic E-layer was experienced following the maximum lightning activity and the effect was more pronounced under night time condition (Barta et al. 2014, submitted).

These researches are related to the activity of the TEA-IS (Thunderstorm Effects on Atmosphere-Ionosphere System) network supported by ESF (European Science Foundation).

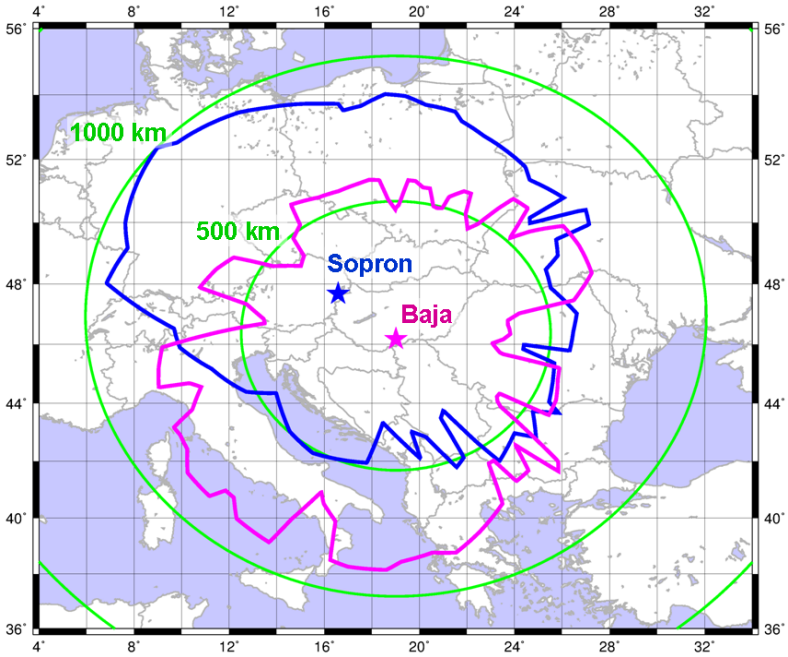

The Universitat Politecnica de Catalunya group (UPC, Barcelona, Spain)

Ongoing activities (related to the ASIM mission)

Observations of TLE from Curaçao: A high-speed video camera system started to operate since May 2014 observing to the southwest direction over Lake Maracaibo and surrounding areas, including Catatumbo (Venezuela). 60 sprites have been recorded with the high speed video camera. A ELF-MF (500 kHz) wide band receiver (U. of Bath, Martin Füllekrug) was installed at the site but had experienced some technical problems.

At the beginning of March 2015, we installed a new magnetometer (0.0001 to 300 Hz) in Cape Verde Islands (LAT: 16.7N, LON: 22.9W). Earle Williams (MIT) participated in the installation of the station, too.

Fig. 1 One of the recorded sprites from Curaçao

Setup of the Colombia Lightning Mapping Array (COLMA): From 10-17 of April 2015, David Romero (UPC) and Jesús López (UNAL and soon UPC too) installed a 6 sensor network in the Santa Marta area in the north of Colombia (Caribbean shore). Currently the network is under test. On 20th of May Jesús López will visit all the sensors in order to evaluate the sites. We thank to Daniel Aranguren and Horacio Torres for their assistance for making this LMA network possible in the tropics.

Fig. 2 Earle Williams during the antenna alignment (Left) and outdoors sensor electronics powered by solar panels (Right).

University of Florida (Gainesville, FL, USA)

Lightning experiments and observations will continue in Summer 2015 at Camp Blanding, Florida (for the 22nd year), as well as at the Lightning Observatory in Gainesville (LOG), located at a distance of about 45 km from Camp Blanding. The two facilities are linked by a dedicated phone line. Additionally, coordinated field measurements will be performed at the Golf Course site, located at a distance of 3 km from the Camp Blanding facility. A Lightning Mapping Array (LMA) will be operated (for the 5th summer) in the Camp Blanding area.

J.T. Pilkey, M.A. Uman, J.D. Hill, T. Ngin, W.R. Gamerota, D.M. Jordan, J. Caicedo, and B. Hare authored a paper titled “Rocket-triggered lightning propagation paths relative to preceding natural lightning activity and inferred cloud charge”. Lightning Mapping Array (LMA) data are used to compare the propagation paths of seven rocket-triggered lightning flashes to the inferred charge structure of the thunderstorms in which they were triggered. This is the first LMA study of Florida thunderstorm charge structure. Three sequentially (within 16 min) triggered lightning flashes, whose initial stages were the subject of Hill et al. (2013), are reexamined by comparing the complete flashes to the preceding natural lightning to demonstrate that the three rocket-triggered flashes propagated through an inferred negative charge region that decreased from about 6.8 to about 4.4 km altitude as the thunderstorm dissipated. Two other flashes were also sequentially triggered (within 9 min) in a thunderstorm that contained a convectively intense region ahead of a stratiform region, with similar observed results. Finally, two unique cases of triggered lightning flashes are presented. In the first case, the in-cloud portion of the triggered lightning flash, after ascending to and turning horizontal at 5.3 km altitude, just above the 0 ℃ level, was observed to very clearly resemble the geometry of the in-cloud portion of the preceding

natural lightning discharges. In the second case, a flash was triggered relatively early in the storm's lifecycle that did not turn horizontal near the 0 ℃ level, as is usually the case for triggered lightning in dissipating storms, but ascended to nearly 7.5 km altitude before exhibiting extensive horizontal branching. The paper is published in the JGR - Atmospheres.

F.L. Carvalho, D.M. Jordan, M.A. Uman, T. Ngin, W.R. Gamerota, and J.T. Pilkey authored a paper titled "Simultaneously measured lightning return stroke channel-base current and luminosity". The time delay between lightning return stroke current and the resultant luminosity was measured for 22 return strokes in eight lightning flashes triggered by the rocket-and-wire technique during the summer of 2014 in Florida. The current-to-luminosity delay measured at the channel base at the 20% amplitude level ranged from 30 to 200 ns with an average of 90 ns and at the 50% amplitude level ranged from 30 to 180 ns with an average of 94 ns. The delays are significantly shorter than that predicted by Liang et al. (2014) from theory. The current-to-luminosity delays increase with increasing current risetime, current risetime varying from 190 ns to 570 ns, but the delay appears not to depend on the peak current value. The paper is published in the GRL.

Y. Chen (spent one year as a visiting scholar at UF), X. Wang, and V.A. Rakov authored a paper titled "Approximate expressions for lightning electromagnetic fields at near and far ranges: Influence of return-stroke speed". The waveforms of lightning return-stroke electromagnetic fields on ground are studied using the transmission line model. Approximate expressions to calculate lightning electromagnetic fields at near and far ranges are presented. It is found that the waveforms of lightning electric and magnetic fields in the time domain at both near and far ranges can be expressed approximately as the channel-base current waveform multiplied by a factor which is a function of the return-stroke speed v and the horizontal distance r between the return-stroke channel and the observation point on ground. The ranges at which the approximate expressions are valid are determined. The ranges of validity increase with increasing the return-stroke speed, and the near and far field approximate expressions converge to the exact formula as the return-stroke speed approaches the speed of light. The paper is published in the JGR - Atmospheres.

Vaisala

The following papers have been recently published by Vaisala in the areas of lightning locating systems, lightning characteristics, and lightning climatology.

Nag, A., M. J. Murphy, W. Schulz, and K. L. Cummins (2015) Lightning locating systems: Insights on characteristics and validation techniques, Earth and Space Science, 2, doi:10.1002/2014EA000051.

Abstract— Ground-based and satellite-based lightning locating systems are the most common ways to detect and geolocate lightning. Depending upon the frequency range of operation, LLSs may report a variety of processes and characteristics associated with lightning flashes including channel formation, leader pulses, cloud-to-ground return strokes, M-components, ICC pulses, cloud lightning pulses, location, duration, peak current, peak radiated power and energy, and full spatial extent of channels. Lightning data from different

types of LLSs often provide complementary information about thunderstorms. For all the applications of lightning data, it is critical to understand the information that is provided by various lightning locating systems in order to interpret it correctly and make the best use of it. In this study, we summarize the various methods to geolocate lightning, both ground-based and satellite-based, and discuss the characteristics of lightning data available from various sources. The performance characteristics of lightning locating systems are determined by their ability to geolocate lightning events accurately with high detection efficiency and with low false detections and report various features of lightning correctly. Different methods or a combination of methods may be used to validate the performance characteristics of different types of lightning locating systems. We examine these methods and their applicability in validating the performance characteristics of different LLS types.

Table 3. Performance Characteristics of Different Types of LLSs That Can Be Validated Using the Different Techniques Discussed in Section 5[a]

	LLS Type			
Validation Technique	Long Range (ELF-VLF)	Medium Range (ELF-HF)	VHF Mapping	Visible and Near Infrared (Satellite Based)
LLS self-reference	Estimated DE (CG stroke, CG flash), estimated LA	Estimated DE (CG stroke, CG flash, IC flash), estimated LA (CG strokes and IC pulses)	Estimated DE (IC flash)	NA
Rocket-triggered lightning and lightning strikes to tall objects	DE (CG stroke), DE (CG flash), LA (CG stroke), polarity and peak current estimation accuracy	DE (CG stroke), DE (CG flash), LA (CG stroke), polarity and peak current estimation accuracy, lightning type classification accuracy	DE (CG flash) approximate LA (CG flash)	DE (CG flash), DE (CG stroke), approximate LA (CG flash)
Video camera measurements	DE (CG stroke), DE (CG flash), DE (IC flash), relative LA (CG subsequent stroke), polarity estimation accuracy (with electric field data)	DE (CG stroke), DE (CG flash), DE (IC flash), relative LA (CG subsequent stroke), polarity estimation accuracy (with electric field data)	DE (CG flash), DE (IC flash)	DE (CG flash), DE (CG stroke), DE (IC flash),
Intercomparison among LLSs	see Table 4	see Table 4	see Table 4	see Table 4

[a]CG = cloud-to-ground, IC = intracloud, NA = not applicable.

Holle, R. L., and M. J. Murphy, 2015: Lightning in the North American Monsoon: An exploratory climatology. *Monthly Weather Review*, **143**, 1970-1977.

Abstract—Temporal and spatial distributions of the North American monsoon have been studied previously with rainfall and satellite data. In the current study, the monsoon is examined with lightning data from Vaisala's Global Lightning Dataset (GLD360). GLD360 has been operating for over three years and provides sufficient data to develop an exploratory climatology with minimal spatial variation in detection efficiency and location accuracy across the North American monsoon region. About 80% of strokes detected by GLD360 are cloud to ground. This paper focuses on seasonal, monthly, and diurnal features of lightning occurrence during the monsoon season from Mazatlán north-northwest to northern Arizona and New Mexico. The goal is to describe thunderstorm frequency with a dataset that provides uniform spatial coverage at a resolution of 2–5 km and uniform temporal coverage with individual lightning events resolved to the millisecond, compared with prior studies that used hourly point rainfall or satellite data with a resolution of several kilometers. The monthly lightning stroke density over northwestern Mexico increases between May and June, as thunderstorms begin over the high terrain east of the Gulf of California. The monthly lightning stroke density over the entire region increases

dramatically to a maximum in July and August. The highest stroke densities observed in Mexico approach those observed by GLD360 in subtropical and tropical regions in Africa, central and South America, and Southeast Asia. The diurnal cycle of lightning exhibits a maximum over the highest terrain near noon, associated with daytime solar heating, a maximum near midnight along the southern coast of the Gulf, and a gradual decay toward sunrise.

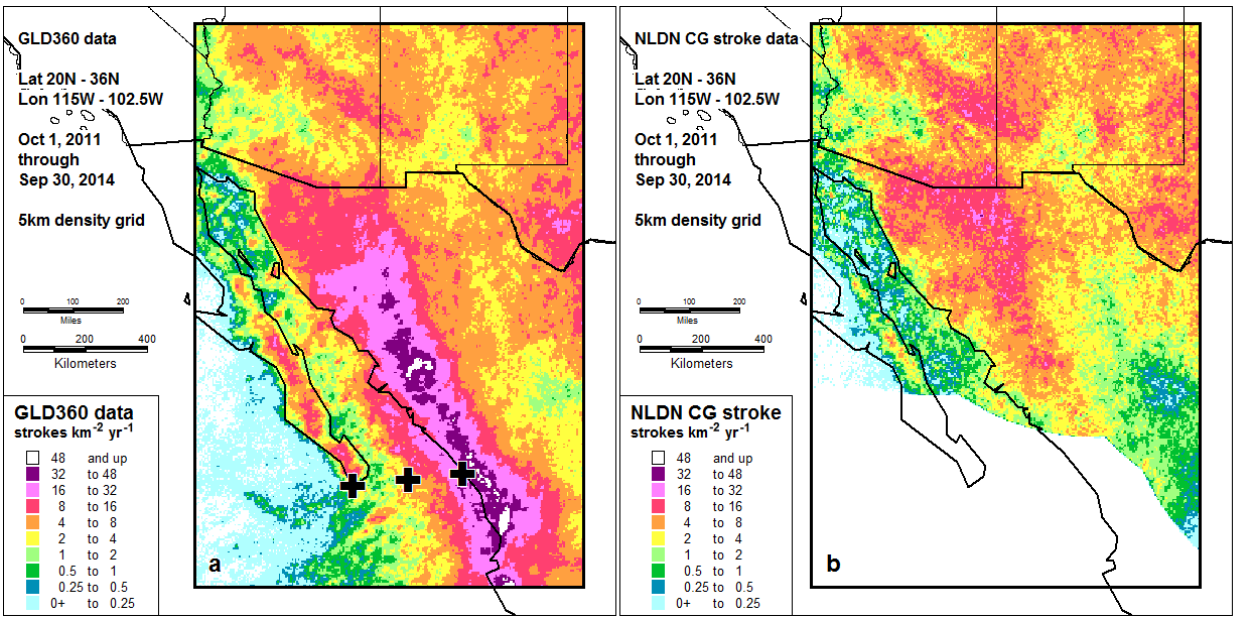

Figure. Lightning stroke density (km^{-2} yr^{-1}) over the area of the North America monsoon detected by (a) GLD360 and (b) NLDN. The scale is on bottom left of each map. A grid size of 5 km by 5km is being used to plot the 45 640 820 strokes detected in the area from October 2011 to September 2014.

RECENT PUBLICATIONS

This list of references is not exhaustive. It includes only papers published during the last six months provided by the authors or found from an on-line research in journal websites. Some references of papers very soon published have been provided by their authors and included in the list. The papers in review process, the papers from Proceedings of Conference are not included.

Ahmad M R, M R M Esa, V Cooray, Z A Baharudin and P Hettiarachchi. 2015. Latitude dependence of narrow bipolar pulse emissions. J. Atmos. Sol-terr. Phy., 128: 40–45.

Anderson J F, J B Johnson, R O Arechiga and R J Thomas. 2014. Mapping thunder sources by inverting acoustic and electromagnetic observations. J. Geophys. Res. Atmos., 119(23): 13,287–13,304.

Andreotti A, A Pierno and V A Rakov. 2015. A new tool for calculation of lightning-induced voltages in power systems – Part II: Validation study. IEEE Trans. on Power Delivery, 30(1): 334–341.

Andreotti A, A Pierno and V A Rakov. 2015. A new tool for calculation of lightning-induced voltages in power systems – Part I: Model development. IEEE Trans. on Power Delivery, 30(1): 326–333.

Antunes L S, A C V Saraiva, O Pinto Jr., J Alves, L Z S Campos, E S A M Luz, C Medeiros and T S Buzato. 2015. Day-to-day differences in the characterization of lightning observed by multiple high-speed cameras. Electr. Pow. Syst. Res., 118: 93–100.

Apel E C, R S Hornbrook, A J Hills, N J Blake, M C Barth, A Weinheimer, C Cantrell, S A Rutledge, B Basarab, J Crawford, G Diskin, C R Homeyer, T Campos, F Flocke, A Fried, D R Blake, W Brune, I Pollack, J Peischl, T Ryerson, P O Wennberg, J D Crounse, A Wisthaler, T Mikoviny, G Huey, B Heikes, D O'Sullivan and D D Riemer. 2015. Upper tropospheric ozone production from lightning NOx-impacted convection: Smoke ingestion case study from the DC3 campaign. J. Geophys. Res. Atmos., 120(6): 2505–2523.

Ávila E E, R E Bürgesser, N E Castellano and M G Nicora. 2015. Diurnal patterns in lightning activity over South America. J. Geophys. Res. Atmos., Article first published online : 17 APR 2015, DOI: 10.1002/2014JD022965.

Baba Y and V A Rakov. 2014. Applications of the FDTD method to lightning electromagnetic pulse and surge simulations. IEEE Trans. on EMC, 56(6): 1506-1521.

Babich L P, E I Bochkov, I M Kutsyk, T Neubert and O Chanrion. 2015. A model for electric field enhancement in lightning leader tips to levels allowing X - and γ - ray emissions. J. Geophys. Res. Space Physics, Accepted manuscript online: 15 APR 2015, DOI: 10.1002/2014JA020923.

Barnes D E, M E Splitt, J R Dwyer, S Lazarus, D M Smith and H K Rassoul. 2015. A study of thunderstorm microphysical properties and lightning flash counts associated with terrestrial gamma-ray flashes. J. Geophys. Res. Atmos., Article first published online : 24 APR 2015, DOI: 10.1002/2014JD021495.

Barta V, M Pietrella, C Scotto, P Bencze, G Sátori. 2014. Thunderstorm - related variations in the ionospheric sporadic E layer. Submitted to Acta Geodaetica et Geophysica Hungarica.

Bates B C, R E Chandler and A J Dowdy. 2015. Estimating trends and seasonality in Australian monthly lightning flash counts. J. Geophys. Res. Atmos., Article first published online : 12 MAY 2015, DOI: 10.1002/2014JD023011.

Bazelyan E M, Y P Raizer and N L Aleksandrov. 2015. The effect of space charge produced by

corona at ground level on lightning attachment to high objects. Atmos. Res., 153: 74–86.

Bech J, J Arús, S Castán, N Pineda, T Rigo, J Montanyà and O van der Velde. 2015. A study of the 21 March 2012 tornadic quasi linear convective system in Catalonia. Atmos. Res., 158–159: 192–209.

Bharali C, B Pathak and P K Bhuyan. 2015. Spring and summer night-time high ozone episodes in the upper Brahmaputra valley of North East India and their association with lightning. Atmospheric Environment, 109: 234–250.

Blaes P R, R A Marshall and U S Inan. 2014. Return stroke speed of cloud-to-ground lightning estimated from elve hole radii. Geophys. Res. Lett., 41(24): 9182–9187.

Bór J, B Brockhauser, M Popek, F Ács, H-D Betz. 2014. Case studies of red sprite producing thunderstorms in Hungary. 2nd TEA-IS Summer School, Collioure, France, 23-27 June, 2014. Abstract appeared in digital (PDF) programme book, 2014 Poster.

Brockhauser B, J Bór, F Ács, M Popek and H-D Betz. 2014. Meteorological characteristics of red sprite producing thunderstorms above Hungary. EGU General Assembly 2014, Vienna, Austria, April 27 - May 02, 2014. Geophysical Research Abstracts, Vol. 16, Abstract No. EGU2014-3444, 2014 Poster.

Campos L Z S, M M F Saba, and E P Krider. 2014. On Beta-2 stepped leaders in negative cloud-to-ground lightning. J. Geophys. Res. Atmos., 119.

Carlson B E, C Liang, P Bitzer and H Christian. 2015. Time domain simulations of preliminary breakdown pulses in natural lightning. J. Geophys. Res. Atmos., Accepted manuscript online: 25 APR 2015, DOI: 10.1002/2014JD022765.

Carvalho F L, D M Jordan, M A Uman, T Ngin, W R Gamerota and J T Pilkey. 2014. Simultaneously measured lightning return stroke channel-base current and luminosity. Geophys. Res. Lett., 41(22): 7799–7805.

Cen J, P Yuan, S Xue and X Wang. 2015. Spectral characteristics of lightning dart leader propagating in long path. Atmos. Res., In Press, Accepted Manuscript, Available online 8 May 2015.

Chang S-C, R-R Hsu, S-M Huang, H-T Su, C-L Kuo, J-K Chou, L-J Lee, Y-J Wu and A B Chen. 2014. Characteristics of TLE-producing lightning in a coastal thunderstorm. J. Geophys. Res. Space Physics, 119(11): 9303–9320.

Chen L, W Lu, Y Zhang and D Wang. 2015. Optical progression characteristics of an interesting natural downward bipolar lightning flash. J. Geophys. Res. Atmos., 120(2): 708–715.

Chen M, T Lu and Y Du. 2015. An improved wave impedance approach for locating close lightning stroke from single station observation and its validation. J. Atmos. Sol-terr. Phy., 122: 1–8.

Chen M, T Lu and Y Du. 2015. Corrigendum to ‘Properties of “site error” of lightning direction-finder (DF) and its modelling’ [Atmos. Res. 129–130 (2013) 97–109]. Atmos. Res., 153: 578.

Chen Y, X Wang and V A Rakov. 2015. Approximate expressions for lightning electromagnetic fields at near and far ranges: Influence of return-stroke speed. J. Geophys. Res. Atmos., 120: 2855–2880.

Chen Y, X Wang and V A Rakov. 2015.

RECENT PUBLICATIONS

Approximate expressions for lightning electromagnetic fields at near and far ranges: Influence of return-stroke speed. J. Geophys. Res. Atmos., 120(7): 2855–2880.

Chronis T, K Cummins, R Said, W Koshak, E McCaul, E R Williams, G T Stano and M Grant. 2015. Climatological diurnal variation of negative CG lightning peak current over the continental United States. J. Geophys. Res. Atmos., 120(2): 582–589.

Conti A D, F H Silveira and S Visacro. 2015. Close electric fields and lightning-induced voltages predicted by a return-stroke model including corona and nonlinear channel resistance. Electr. Pow. Syst. Res., 118: 8–14.

Cummer S A, M S Briggs, J R D, S Xiong, V Connaughton, G J Fishman, G Lu, F Lyu and R Solanki. 2014. The source altitude, electric current, and intrinsic brightness of terrestrial gamma ray flashes. Geophys. Res. Lett., 41(23): 8586–8593.

Dommain R, A R Cobb, H Joosten, P H Glaser, A F L Chua, L Gandois, F-M Kai, A Noren, K A Salim, N S H Su'ut and C F Harvey. 2015. Forest dynamics and tip-up pools drive pulses of high carbon accumulation rates in a tropical peat dome in Borneo (Southeast Asia). J. Geophys. Res. Biogeosciences, Article first published online : 15 APR 2015, DOI: 10.1002/2014JG002796.

Dyrda M, A Kulak, J Mlynarczyk, M Ostrowski, J Kubisz, A Michalec and Z Nieckarz. 2014. Application of the Schumann resonance spectral decomposition in characterizing the main African thunderstorm center. J. Geophys. Res. Atmos., 119(23): 13,338–13,349.

Fabró F, J Montanyà, M Marisaldi, O A van der Velde and F Fuschino. 2015. Analysis of global Terrestrial Gamma Ray Flashes distribution and special focus on AGILE detections over South America. J. Atmos. Sol-terr. Phy., 124: 10–20.

Fatichi S, P Molnar, T Mastrotheodoros and P Burlando. 2015. Diurnal and seasonal changes in near-surface humidity in a complex orography. J. Geophys. Res. Atmos., 120(6): 2358–2374.

Fedorov E, A Schekotov, Y Hobara, R Nakamura, N Yagova and M Hayakawa. 2014. The origin of spectral resonance structures of the ionospheric Alfvén resonator. Single high-altitude reflection or resonant cavity excitation? J. Geophys. Res., 119(4): 3117–3129.

Fraser-Smith A C and S N Kjono. 2014. The ULF magnetic fields generated by thunderstorms: A source of ULF geomagnetic pulsations? Radio Sci., 49(12): 1162–1170.

Gamerota W R, M A Uman, J D Hill and D M Jordan. 2015. Observations of corona in triggered dart-stepped leaders. Geophys. Res. Lett., 42(6): 1977–1983.

Gamerota W R, M A Uman, J D Hill, T Ngin, J Pilkey and D M Jordan. 2015. Estimation of triggered-lightning dart-stepped-leader currents from close multiple-station dE/dt pulse measurements. J. Geophys. Res. Atmos., 120(4): 1458–1475.

Ghodpage R N, A Taori, P T Patil1, D Siingh, S Gurubaran, A K Sharma. 2015. On the vertical wavelength estimates using the Krassovsky parameters of OH airglow monitoring. Current Science, 108: 1362-1369.

Giannaros T M, V Kotroni and K Lagouvardos. 2015. Predicting lightning activity in Greece with the Weather Research and Forecasting (WRF) model. Atmos. Res., 156: 1–13.

Halder M, A Hazra, P Mukhopadhyay, D Siingh.

RECENT PUBLICATIONS

2014. Effect of the better representation of the cloud ice-nucleation in WRF microphysics schemes: A case study of a severe storm in India. Atmos. Res., 154: 155-174.

He J, X Zhang, P Yang, S Chen and R Zeng. 2015. Attenuation and deformation characteristics of lightning impulse corona traveling along bundled transmission lines. Electr. Pow. Syst. Res.,, 118: 29–36.

Heidler F, A Piantini and M Rubinstein. 2015. Special Issue "The Lightning Flash and Lightning Protection" (XII SIPDA 2013). Electr. Pow. Syst. Res., 118:1–2.

Jánský J and V P Pasko. 2014. Charge balance and ionospheric potential dynamics in time-dependent global electric circuit model. J. Geophys. Res. Space Physics, 119(12): 10,184–10,203.

Jurković P M, N S Mahović and D Počakal. 2015. Lightning, overshooting top and hail characteristics for strong convective storms in Central Europe. Atmos. Res., 161–162: 153–168.

Kamra A K and A A Nair. 2015. The impact of the Western Ghats on lightning activity on the western coast of India. Atmos. Res., 160: 82–90.

Karunarathne S, T C Marshall, M Stolzenburg, N Karunarathna and R E Orville. 2015. Modeling stepped leaders using a time-dependent multidipole model and high-speed video data. J. Geophys. Res. Atmos., 120(6): 2419–2436.

Kawabata T, S Yanagawa, H Takahashi and K Yamamoto. 2015. Development of a shunt lightning current measuring system using a Rogowski coil. Electr. Pow. Syst. Res., 118: 110–113.

Kiszely M, J Bór, P Mónus and H-D Betz. 2014. Signatures of lightning activity in seismic records. EGU General Assembly 2014, Vienna, Austria, April 27 - May 02, 2014. Geophysical Research Abstracts, Vol. 16, Abstract No. EGU2014-3416, 2014 Poster.

Kocifaj M, G Videen and J Klačka. 2015. Backscatter in a cloudy atmosphere as a lightning-threat indicator. J. Quant. Spectrosc. Ra., 150: 175–180.

Kong X, Y Zhao, T Zhang and H Wang. 2015. Optical and electrical characteristics of in-cloud discharge activity and downward leaders in positive cloud-to-ground lightning flashes. Atmos. Res., 160: 28–38.

Kulkarni M N. 2015. A new tool for predicting drought: An application over India. Scientific Reports, 5: 1–8, DOI:10.1038/srep07680.

Köhn C and U Ebert. 2015. Calculation of beams of positrons, neutrons, and protons associated with terrestrial gamma ray flashes. J. Geophys. Res. Atmos., 120(4): 1620–1635.

Lang T J, S A Cummer, D Petersen, L Flores-Rivera, W A Lyons, D MacGorman and W Beasley. 2015. Large charge moment change lightning on 31 May to 1 June 2013, including the El Reno tornadic storm. J. Geophys. Res. Atmos., Article first published online : 17 APR 2015, DOI: 10.1002/2014JD022600.

Lapierre J L, R G Sonnenfeld, H E Edens and M Stock. 2014. On the relationship between continuing current and positive leader growth. J. Geophys. Res. Atmos., 119(22): 12,479–12,488.

Lorenz R D and D J Lawrence. 2015. Gamma rays and cosmic rays at Venus: The Pioneer Venus gamma ray detector and considerations for future measurements. Planetary and Space Science, 109–110: 129–134.

RECENT PUBLICATIONS

Lowke J J. 2015. The initiation of lightning in thunderclouds: The possible influence of metastable nitrogen and oxygen molecules in initiating lightning streamers. J. Geophys. Res. Atmos., Article first published online : 21 APR 2015, DOI: 10.1002/2014JD022223.

Lu G, R Jiang, X Qie, H Zhang, Z Sun, M Liu, Z Wang and K Liu. 2014. Burst of intracloud current pulses during the initial continuous current in a rocket-triggered lightning flash. Geophys. Res. Lett., 41(24): 9174–9181.

Lyu F, S A Cummer, R Solanki, J Weinert, L McTague, A Katko, J Barrett, L Zigoneanu, Y Xie and W Wang. 2014. A low-frequency near-field interferometric-TOA 3-D Lightning Mapping Array. Geophys. Res. Lett., 41(22): 7777–7784.

Mallick S, V A Rakov, J D Hill, T Ngin, W R Gamerota, J T Pilkey, D M Jordan, M A Uman, S Heckman, C D Sloop and C Liu. 2015. Performance characteristics of the ENTLN evaluated using rocket-triggered lightning data. Electr. Pow. Syst. Res., 118: 15–28.

Mareev E A and E M Volodin. 2014. Variation of the global electric circuit and Ionospheric potential in a general circulation model. Geophys. Res. Lett., 41(24): 9009–9016.

Marshall T, M Stolzenburg, N Karunarathna and S Karunarathne. 2014. Electromagnetic activity before initial breakdown pulses of lightning. J. Geophys. Res. Atmos., 119(22): 12,558–12,574.

Mlynarczyk J, J Bór, A Kulak, M Popek and J Kubisz. 2015. An unusual sequence of sprites followed by a secondary TLE: An analysis of ELF radio measurements and optical observations. J. Geophys. Res. Space Physics, 120(3): 2241–2254.

Mlynarczyk J, J Bór, A Kulak, M Popek, J Kubisz. 2014. An unusual sequence of sprites followed by a troll – an analysis of ELF radio measurements and optical observations. Submitted to J. Geophys. Res. Space Physics, 2014.

Mourenas D, A V Artemyev, O V Agapitov, V Krasnoselskikh and W Li. 2014. Approximate analytical solutions for the trapped electron distribution due to quasi-linear diffusion by whistler mode waves. J. Geophys. Res. Space Physics, 119(12): 9962–9977.

Nag A and V A Rakov. 2015. A transmission-line-type model for lightning return strokes with branches. Electr. Pow. Syst. Res., 118: 3–7.

Nag A, M J Murphy, W Schulz and K L Cummins. 2015. Lightning locating systems: Insights on characteristics and validation techniques. Earth and Space Science, 2(4): 65–93.

Nickolaenko A P and M Hayakawa. 2014. Spectra and waveforms of ELF transients in the Earth-ionosphere cavity with small losses. Radio Sci., 49(2): 118–130.

Nickolaenko A P, A Yu Schekotov, M Hayakawa, Y Hobara, G S´atori, J Bor and M Neska. 2014. Multi-point detection of the ELF transient caused by the gamma flare of December 27, 2004. Radiophysics and Quantum Electronics, 57(2): 125–140.

Nieckarz Z, P Baranski, J Mlynarczyk, A Kulak and J Wiszniowski. 2015. Comparison of the charge moment change calculated from electrostatic analysis and from ELF radio observations. J. Geophys. Res. Atmos., 120(1): 63–72.

Nishihashi M, K Arai, C Fujiwara, W Mashiko, S Yoshida, S Hayashi and K Kusunoki. 2015. Characteristics of lightning jumps associated with a tornadic supercell on 2

September 2013. SOLA, 11: 18−22.

Odzimek A, M Pajek, J Bór, P Struzik, P Novak, M Mielniczek and M Popek. 2014. Optical observations of sprites supported by OST images. 22nd Cartographic School, Geoinformatics and Atmospheric Science, Wałbrzych-Książ, Poland, 06–09 May, 2014. Page 47 of abstract book, 2014, Poster.

Pan L L, C R Homeyer, S Honomichl, B A Ridley, M Weisman, M C Barth, J W Hair, M A Fenn, C Butler, G S Diskin, J H Crawford, T B Ryerson, I Pollack, J Peischl and H Huntrieser. 2014. Thunderstorms enhance tropospheric ozone by wrapping and shedding stratospheric air. Geophys. Res. Lett., 41(22): 7785–7790.

Pilkey J T, M A Uman, J D Hill, T Ngin, W R Gamerota, D M Jordan, J Caicedo and B Hare. 2014. Rocket-triggered lightning propagation paths relative to preceding natural lightning activity and inferred cloud charge. J. Geophys. Res. Atmos., 119(23): 13,427–13,456.

Qin J and V P Pasko. 2015. Dynamics of sprite streamers in varying air density. Geophys. Res. Lett., 42(6): 2031–2036.

Quiquet A, A T Archibald, A D Friend, J Chappellaz, J G Levine, E J Stone, P J Telford and J A Pyle. 2015. The relative importance of methane sources and sinks over the Last Interglacial period and into the last glaciation. Quaternary Science Reviews, 112: 1–16.

Rakov V A. 2015. CIGRE technical brochure on lightning parameters for engineering applications. Electricity, 1: 61-64.

Ripoll J-F, J M Albert and G S Cunningham. 2014. Electron lifetimes from narrowband wave-particle interactions within the plasmasphere. J. Geophys. Res. Space Physics, 119(11): 8858–8880.

Ripoll J-F, Y Chen, J F Fennell and R H W Friedel. 2015. On long decays of electrons in the vicinity of the slot region observed by HEO3. J. Geophys. Res. Space Physics, 120(1): 460–478.

Rozhnoi A, M Solovieva, B Levin, M Hayakawa and V Fedun. 2014. Meteorological effects in the lower ionosphere as based on VLF/LF signal observations. Natural Hazards Earth System Sci., 14: 2671–2679.

Saba M M F, C Schumann, T A Warner, J H Helsdon and R E Orville. 2015. High-speed video and electric field observation of a negative upward leader connecting a downward positive leader in a positive cloud-to-ground flash. Electr. Pow. Syst. Res., 118: 89–92.

Sadighi S, N Liu, J R Dwyer and H K Rassoul. 2015. Streamer formation and branching from model hydrometeors in subbreakdown conditions inside thunderclouds. J. Geophys. Res. Atmos., Article first published online : 6 MAY 2015, DOI: 10.1002/2014JD022724.

Sato M, T Ushio, T Morimoto, M Kikuchi, H Kikuchi, T Adachi, M Suzuki, A Yamazaki, Y Takahashi, U Inan, I Linscott, R Ishida, Y Sakamoto, K Yoshida, Y Hobara, T Sano, T Abe, M Nakamura, H Oda and Z-I Kawasaki. 2015. Overview and early results of the Global Lightning and Sprite Measurements mission. J. Geophys. Res. Atmos., Article first published online: 11 MAY 2015, DOI: 10.1002/2014JD022428.

Selvakumaran R, A K Maurya, S A Gokani, BVeenadhari, S Kumar, K Venkatesham, D V Phanikumar, A K Singh, D Siingh, R Singh. 2015. Solar flares induced D-region ionospheric and geomagnetic perturbations. J. Atmos. Sol-terr. Phy., 123: 102-112.

Shmatov M L. 2015. New model of initial

acceleration of electrons of terrestrial gamma-ray flashes with a hard spectrum. Physics Letters A, 379(20–21): 1358–1360.

Shvets A V, T M Serdiuk, Y V Gorishnyaya, Y Hobara and M Hayakawa. 2014. Estimating the lower ionosphere height and lightning location using multimode “tweek” atmospherics. J. Atmos. Solar-terr. Phys., 108: 1–9.

Siingh D, P S Buchunde, H Gandhi, R Singh, S Singh, M N Patil and R P Singh. 2015. Lightning and convective rain over Indian peninsula and Indo-China peninsula. Adv. Space Res., 55(4): 1085–1103.

Silva C L da and V P Pasko. 2015. Physical mechanism of initial breakdown pulses and narrow bipolar events in lightning discharges. J. Geophys. Res. Atmos., Accepted manuscript online: 15 APR 2015, DOI: 10.1002/2015JD023209.

Sima W, Y Li, V A Rakov, Q Yang, T Yuan, and M Yang. 2014. An analytical method for estimation of lightning performance of transmission lines based on a leader progression model. IEEE Trans. on EMC, 56(6): 1530-1539.

Singh B, R Tyagi, Y Hobara and M Hayakawa. 2014. X-rays and solar proton event induced changes in the first mode Schumann resonance frequency observed at a low latitude station Agra, India. J. Atmos. Solar-terr. Phys.,113: 1–9.

Singh R, D Siingh, S A Gokani, P S Buchunde, R P Singh, A K Singh. 2015. Climate, topographical and meteorological investigation of 16-17 June 2013 Kedarnath (India) disaster causes. Natural Hazards and Earth System Science Discussions, 3 February 2015, DOI:10.5194/nhessd-3-941-2015, 941–953.

Skeltved A B, N Østgaard, B Carlson, T Gjesteland and S Celestin. 2014. Modeling the relativistic runaway electron avalanche and the feedback mechanism with GEANT4. J. Geophys. Res. Space Physics, 119(11): 9174–9191.

Smirnov S. 2014. Reaction of electric and meteorological states of the near-ground atmosphere during a geomagnetic storm on 5 April 2010. Earth, Planets and Space, 66:154. doi: 10.1186/s40623-014-0154-2.

Sorokin V and M Hayakawa. 2014. Plasma and electromagnetic effects caused by the seismic-related disturbances of electric current in the global circuit. Modern Appl. Sci., 8(4): 61–83.

Stolzenburg M, T C Marshall, S Karunarathne, N Karunarathna and R E Orville. 2015. Transient luminosity along negative stepped leaders in lightning. J. Geophys. Res. Atmos., Article first published online: 24 APR 2015, DOI: 10.1002/2014JD022933.

Stolzenburg M, T C Marshall, S Karunarathne, N Karunarathna and R E Orville. 2014. Leader observations during the initial breakdown stage of a lightning flash. J. Geophys. Res. Atmos., 119(21): 12,198–12,221.

Sun Z, X Qie, R Jiang, M Liu, X Wu, Z Wang, G Lu and H Zhang. 2014. Characteristics of a rocket-triggered lightning flash with large stroke number and the associated leader propagation. J. Geophys. Res. Atmos., 119(23): 13,388–13,399.

Thang T H, Y Baba, N Nagaoka, A Ametani, N Itamoto and V A Rakov. 2015. FDTD simulation of direct lightning strike to a phase conductor: Influence of corona on transient voltages at the tower. Electric Power Systems

Research, 123: 128–136.

Ushio T, T Wu and S Yoshida. 2015. Review of recent progress in lightning and thunderstorm detection techniques in Asia. Atmos. Res., 154: 89-102.

Wapler K and P James. 2015. Thunderstorm occurrence and characteristics in Central Europe under different synoptic conditions. Atmos. Res., 158–159: 231–244.

Vavilov D I and D R Shklyar. 2014. Ionospherically reflected proton whistlers. J. Geophys. Res. Space Physics, 119(12): 9978–9991.

Velde O A van der, J Montanyà, S Soula, N Pineda and J Mlynarczyk. 2014. Bidirectional leader development in sprite-producing positive cloud-to-ground flashes: Origins and characteristics of positive and negative leaders. J. Geophys. Res. Atmos., 119(22): 12,755–12,779.

Wendel J. 2014. Lightning strikes predicted to increase as climate warms. Eos, 95(47): 431.

Whittaker I C, E Douma, C J Rodger and T J C H Marshall. 2015. A quantitative examination of lightning as a predictor of peak winds in tropical cyclones. J. Geophys. Res. Atmos., Article first published online: 8 MAY 2015, DOI: 10.1002/2014JD022868.

Vodopiyanov I B, J R Dwyer, E S Cramer, R J Lucia and H K Rassoul. 2015. The effect of direct electron-positron pair production on relativistic feedback rates. J. Geophys. Res. Space Physics, 120(1): 800–806.

Vujević S and D Lovrić. 2015. On continuous numerical Fourier transform for transient analysis of lightning current related phenomena. Electr. Pow. Syst. Res., 119: 364–369.

Xu L, Y Zhang, F Wang, et al. 2014. Simulation of the electrification of a tropical cyclone using the WRF-ARW model: An idealized case J. Meteor. Res., 28(3): 453–468.

Xu W and E J Zipser. 2015. Convective intensity, vertical precipitation structures, and microphysics of two contrasting convective regimes during the 2008 TiMREX. J. Geophys. Res. Atmos., Article first published online: 12 MAY 2015, DOI: 10.1002/2014JD022927.

Xu W, S Celestin and V P Pasko. 2015. Optical emissions associated with terrestrial gamma ray flashes. J. Geophys. Res. Space Physics, 120(2): 1355–1370.

Xue S, P Yuan, J Cen, Y Li and X Wang. 2015. Spectral observations of a natural bipolar cloud-to-ground lightning. J. Geophys. Res. Atmos., 120(5): 1972–1979.

Yair Y, C Price, D Katzenelson, N Rosenthal, L Rubanenko, Y Ben-Ami and E Arnone. 2015. Sprite climatology in the Eastern Mediterranean Region. Atmos. Res., 157: 108–118.

Yang J, G Lu, L-J Lee and G Feng. 2015. Long-delayed bright dancing sprite with large Horizontal displacement from its parent flash. J. Atmos. Sol-terr. Phy., 129:1–5.

Yoshida S, T Wu, T Ushio, K Kusunoki and Y Nakamura. 2014. Initial results of LF sensor network for lightning observation and characteristics of lightning emission in LF band. J. Geophys. Res. Atmos., 119(21): 12,034–12,051.

Yue J and W A Lyons. 2015. Structured elves: Modulation by convectively generated gravity waves. Geophys. Res. Lett., 42(4): 1004–1011.

Zhang W, Y Zhang, D Zheng, F Wang and L Xu. 2015. Relationship between lightning activity

and tropical cyclone intensity over the northwest Pacific. J. Geophys. Res. Atmos., Article first published online: 14 MAY 2015, DOI: 10.1002/2014JD022334.

Zhang Y, H Li, Z Wang and W Zhang, J Li. 2015. A preliminary study on time series forecast of fair-weather atmospheric electric field with WT-LSSVM method. J. Electrostat., 75: 85–89.

Zhang Y, S Yang, W Lu, et al. 2014. Experiments of artificially triggered lightning and its application in Conghua, Guangdong, China. Atmos. Res., 135-136: 330–343.

Zhang Y, Y Zhang, D Zheng and W Lu. 2015. Preliminary breakdown, following lightning discharge processes and lower positive charge region. Atmos. Res., 161–162: 52–56.

Zhou H and X Qiao. 2015. Studies of the variations of the first Schumann resonance frequency during the solar flare on 7 March 2012. J. Geophys. Res. Atmos., Accepted manuscript online: 29 APR 2015, DOI: 10.1002/2014JD022696.

Zhou H, V A Rakov, G Diendorfer, R Thottappillil, H Pichler and M Mair. 2015. A study of different modes of charge transfer to ground in upward lightning. Atmos. Sol-terr. Phy., 125–126: 38–49.

Zhou M, D Wang, J Wang, N Takagi, W R Gamerota, M A Uman, D M Jordan, J T Pilkey and T Ngin. 2014. Correlation between the channel-bottom light intensity and channel-base current of a rocket-triggered lightning flash. J. Geophys. Res. Atmos., 119(23): 13,457–13,473.

Zhou W, Y Zhang, Y Zhang, et al. 2014. Occurrence regularity of CPT discharge event in negative cloud-to-ground lightning. Acta Phys. Sin. 63(1), DOI: 10.7498/aps.63.019202.

Reminder

Newsletter on Atmospheric Electricity presents twice a year (May and November) to the members of our community with the following information:

- ✧ announcements concerning people from atmospheric electricity community, especially awards, new books...,
- ✧ announcements about conferences, meetings, symposia, workshops in our field of interest,
- ✧ brief synthetic reports about the research activities conducted by the various organizations working in atmospheric electricity throughout the world, and presented by the groups where this research is performed, and
- ✧ a list of recent publications. In this last item will be listed the references of the papers published in our field of interest during the past six months by the research groups, or to be published very soon, that wish to release this information, but we do not include the contributions in the proceedings of the Conferences.

No publication of scientific paper is done in this Newsletter. We urge all the groups interested to submit a short text (one page maximum with photos eventually) on their research, their results or their projects, along with a list of references of their papers published during the past six months. This list will appear in the last item. Any information about meetings, conferences or others which we would not be aware of will be welcome.

Newsletter on Atmospheric Electricity is now routinely provided on the web site of ICAE (http://www.icae.jp), and on the web site maintained by Monte Bateman http://ae.nsstc.uah.edu/.

ICAE

In order to make our news letter more attractive and informative, it will be appreciated if you could include **up to two photos or figures** in your contribution!

Call for contributions to the newsletter

All issues of this newsletter are open for general contributions. If you would like to contribute any science highlight or workshop report, please contact Daohong Wang (wang@gifu-u.ac.jp) preferably by e-mail as an attached word document. The deadline for **2015 winter** issue of the newsletter is **Nov 15, 2015**.

Editor:
Daohong Wang
Secretary of ICAE
E-mail:wang@gifu-u.ac.jp
Tel: 81-58-293-2702
Fax: 81-58-232-1894

Compiler:
Wenjuan Zhang
Laboratory of Lightning Physics and Protection Engineering
Beijing, China
zhangwj@cams.cma.gov.cn

Newsletters on Atmospheric Electricity are supported by International Commission on Atmospheric Electricity, IUGG/IAMAS.

©2015